ADDIS ABABA UNIVERSITY

SCHOOL OF GRADUATE STUDIES

FACULTY OF TECHNOLOGY

ELECTRICAL AND COMPUTER ENGINEERING

DEPARTMENT

# COMPARATIVE STUDY ON BANDWIDTH ENHANCEMENT TECHNIQUES OF MICROSTRIP PATCH ANTENNA

By

Zewdu Hailu

A thesis submitted to the school of Graduate studies of Addis Ababa University in partial fulfillment of the requirements for the degree of

**Masters of Science in Electrical Engineering**

**(Communication Engineering)**

January 2008

Addis Ababa, Ethiopia

ADDIS ABABA UNIVERSITY

SCHOOL OF GRADUATE STUDIES

FACULTY OF TECHNOLOGY

DEPARTMENT OF ELECTRICAL AND COMPUTER

ENGINEERING

# COMPARATIVE STUDY ON BANDWIDTH ENAHANCEMENT TECHNIQUES OF MICROSTRIP PATCH ANTENNA

By

Zewdu Hailu

Advisor

Dr. Ing. Mohammed Abdo

ADDIS ABABA UNIVERSITY

SCHOOL OF GRADUATE STUDIES

FACULTY OF TECHNOLOGY

# COMPARATIVE STUDY ON BADWIDTHENHANCEMENT TECHNIQUES OF MICROSTRIP PATCH ANTENNA

By

Zewdu Hailu

## APPROVAL BY BOARD OF EXAMINERS

______________________ ______________

Chairman Dept. of Graduate Committee Signature

Dr. Ing. Mohammed Abdo ______________

Advisor Signature

Prof. Woldegiorgis Weldemariam ________________

Internal Examiner Signature

Dr Ing. Hailu Ayele

_________________

External Examiner Signature

## ACKNOWLEDGEMENTS

I lack words, how to express my respect for my father who used to inspire me from my childhood by giving his precious advice to get me learned. It is my pleasure to acknowledge the rest of my family also.

I would like to express my gratitude to Dr. Ing. Mohammed Abdo, my advisor, who was willing to supervise my thesis and creating suitable working environment especially in the laboratory together with sharing his invaluable knowledge and suggestions.

I would like also to thank Mr. Mulugeta A. & Mr. Ashenafi Y. for their constructive ideas and comments.

## Contents

**List of Figures**

## List of Constants and Symbols

$c = 3\times10^{8}\ meters/\sec ond$ $\quad$ $c = velocity\ of\ wave\ in\ free\ space$

$\varepsilon_0 = \frac{1}{36\pi}\times10^{-12}\ Farads/meter$ $\quad$ $\varepsilon_0 = permittivity\ of\ free\ space$

$\mu_0 = 4\pi\times10^{-7}\ Henry/meter$ $\quad$ $\mu_0 = permeability\ of\ free\ space$

$\eta_0 = \sqrt{\frac{\mu_0}{\varepsilon_0}} = 120\pi\ ohms$ $\quad$ $\eta_0 = \text{int}\,rinsic\ impedance$

$\varepsilon_r = relative\ permittivity$

$\mu_r = relative\ permeability$

## List of Acronyms

BW ……………………………………Bandwidth

DRSA…………………………………..Digital Audio Radio Satellite

EMC……………………………………Electromagnetic Coupling

MoM……………………………………Method of Moments

MMIC…………………………………..Monolithic Microwave Integrated Circuits

MSA…………………………………… Microstrip Antenna

PTFE……………………………………Poly tetra-fluoro-ethylene

RF……………………………………… Radio Frequency

RL……………………………………… Return Loss

TE……………………………………… Transverse Electric

TEM……………………………………Transverse Electromagnetic mode

TL………………………………………Transmission Line

TM………………………………………Transverse Magnetic

VSWR…………………………………...Voltage Standing Wave Ratio

WIFI……………………………………..Wireless Fidelity

WLAN…………………………………...Wireless Local Area Networks

# Abstract

Conventional microstrip antennas in general have the attractive features such as low profile, light weight, easy fabrication, and conformability to mounting hosts. However, microstrip antennas inherently have a narrow bandwidth, low gain, and bandwidth enhancement is usually demanded for practical applications. In addition, applications in present-day mobile communication systems usually require smaller antenna size in order to meet the miniaturization requirements of mobile units. Thus, size reduction and bandwidth enhancement are becoming major design considerations for practical applications of microstrip antennas. For this reason, conducting studies to achieve compact and broadband operations of microstrip antennas is thought to be very important. The purpose of this thesis is to make a comparative study on the techniques that help to overcome the bandwidth constraint of microstrip patch antennas and to propose the better technique by taking different consideration such as the antenna gain, bandwidth and related issues. In this thesis work broad banding techniques like using feeding techniques (proximity coupled), stacked patches, parasitic arrangement of patches and the use of different shapes (i.e. E-shaped) are studied. The bandwidth obtained for each type of the antenna are 10.8%, 11.5%, 15.6% and 25.6% respectively with respect to the operating frequency of each of the antennas. The result shows that the E-shaped patch antenna has better performance.

**Key Words**: patch antenna, return loss, bandwidth, gain

# Chapter 1

## Thesis Overview

### 1.1 Introduction

In recent years, the current trend in commercial and government communication systems has been to develop low cost, minimal weight, low profile antennas that are capable of maintaining high performance over a large spectrum of frequencies. This technological trend has focused much effort into the design of microstrip (patch) antennas. With a simple geometry, patch antennas offer many advantages not commonly exhibited in other antenna configurations. For example, they are extremely low profile, lightweight, simple and inexpensive to fabricate using modern day printed circuit board technology, compatible with microwave and millimeter-wave integrated circuits (MMIC), and have the ability to conform to planar and non-planar surfaces. In addition, once the shape and operating mode of the patch are selected, designs become very versatile in terms of operating frequency, polarization, pattern, and impedance. The variety in design that is possible with microstrip antennas probably exceeds that of any other type of antenna element.

### 1.2 Thesis Motivation

Despite the many advantages of patch antennas, they do have some considerable drawbacks. One of the main limitations with patch antennas is their inherently narrowband performance due to its resonant nature. With bandwidths as low as a few percent, broadband applications using conventional patch designs are limited. Other characteristics of patch antennas include low efficiencies, limited power capacity, spurious feed radiation, poor polarization purity, and manufacturing tolerance problems.

For over two decades, research scientists have developed several methods to increase the bandwidth of a patch antenna. Many of these techniques involve adjusting the placement and/or type of element used to feed (or excite) the antenna. The first, simplest and most direct, approach is to increase the thickness of the substrate, while using a low dielectric substrate. Using thick dielectric substrate material on the other hand has the ability to produce undesired surface wave which likely reduces the antenna efficiency, gain, bandwidth, increases the side-lobes and antenna loss in general. The second technique to increase bandwidth is decreasing the relative permittivity, which has an obvious limitation based on size. Therefore, there should be different techniques that are capable to reduce the surface wave excitation while keeping the antenna parameters at the desired level.

## 1.3 Objective of the Thesis

The objective of this thesis is to solve the problem mentioned in the thesis motivation section. To overcome the bandwidth problem, different bandwidth enhancement techniques have been adopted. The most commonly used techniques are proximity coupled patches, parasitic patches, stacked patches, aperture fed patches, log periodic arrangement and other shapes (for example an E-shaped patch, circular annulus). Four of the techniques listed above were selected for this thesis (Chapter 5). Finally based on the results obtained the best technique will be recommended.

## 1.4 Literature Review and Methodology

The invention of microstrip patch antennas has been attributed to several authors, but it was certainly dates in the 1960s with the first works published by Deschamps, Greig and Engleman, and Lewin, among others. After the 1970's research publications started to flow with the appearance of the first design equations. Since then different authors started investigations on microstrip patch antennas like James Hall and David M. Pozar and there are also some who contributed a lot. Throughout the years, authors have dedicated their investigations to creating new designs or variations to the original antenna that, to some extent; produce either wider bandwidths or multiple-frequency operation in a single element. However, most of these innovations bear disadvantages related to the size, height or overall volume of the single element and the improvement in bandwidth suffers usually from a degradation of the other characteristics. It is the purpose of this thesis to introduce the general techniques produced to improve the narrow bandwidth characteristic of patch antennas.

The thesis work is done using a High frequency Electromagnetic simulator called *SONNET*. In order to obtain the required result the important parameters need to be passed correctly. Better results may be obtained after several iteration steps. The simulator is obtained from Sonnet Software Inc.

## 1.5 Thesis Contribution

Microstrip antenna structures are the most common option used to realize millimeter wave monolithic microwave integrated circuits, radar and communication systems. Due to its many advantages over the conventional antenna, the microstrip antenna have achieved importance and generated interest to antenna designers for many years. But the inherent bandwidth problem limits its wide use.

This thesis points out and makes detailed study on some of the techniques available to overcome this bottleneck. The study definitely underlines those techniques that can be applied in any type of microstrip antenna. The antenna designed in this thesis work can be used in wireless local area networks (*WLAN*).

## 1.6 Thesis Outline

The outline of this thesis is as follows.

Chapter 2 provides a brief technical description of microstrip antennas focusing on basic characteristics and typical excitation (feeding) methods, and concludes with an analytical model of a patch. Some of the parameters which are influential in the project are also reassessed and the mathematical expressions are also derived.

Chapter 3 deals mainly with the design a microstrip patch antenna and its basic characteristics such as narrow bandwidth and low gain.

Chapter 4 introduces the different broad-banding techniques that help to overcome the bandwidth limitation of microstrip patch antenna.

Chapter 5 gives a brief explanation of the Sonnet Software used as a simulator and the simulation results obtained for each type of patch antennas under consideration.

Chapter 6 concludes this thesis with a discussion of the results obtained for those antennas and the future works that may be carried on.

# Chapter 2

## Microstrip Antennas

In this following section, the important features of microstrip patch antennas are provided and its principle of operation is explained. Next, some critical performance parameters of patch antennas are discussed.

### 2.1 Introduction

Microstrip antennas are one of the most widely used types of antennas in the microwave frequency range, and they are often used in the millimeter-wave frequency range as well. (Below approximately 1 GHz, the size of a microstrip antenna is usually too large to be practical, and other types of antennas such as wire antennas dominate). Microstrip patch antenna consists of a patch of metal that is placed on the top of a grounded dielectric substrate of thickness *h*, with relative permittivity and permeability $\varepsilon_r$ and $\mu_r$ as shown in Figure 2.1 (usually $\mu_r$=1). The metallic patch may be of various shapes [1], with rectangular and circular being the most common, as shown in Figure 2.2. Most of the discussion in this section will be limited to the rectangular patch, although the basic principles are the same for the circular patch. (Many of the CAD formulas presented will apply approximately for the circular patch if the circular patch is modeled as a square patch of the same area.)

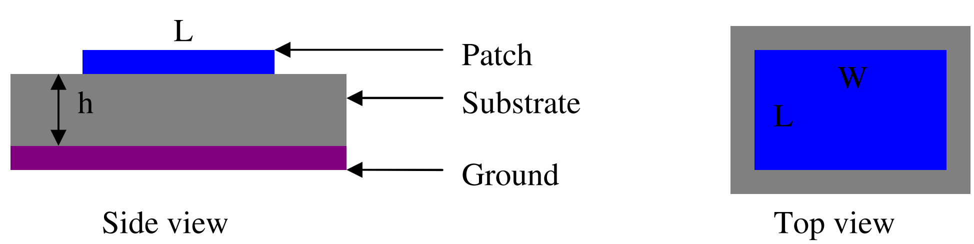


**Figure 2. 1 Lay out of MSA**

#### 2.1.1 Features of Microstrip Antennas

A microstrip antenna consists of a radiating metallic patch or an array of patches situated on one side of a thin, non-conducting, substrate panel with a metallic ground plane situated on the other side of the panel. The metallic patch is normally made of thin copper foil or is copper-foil-plated with a corrosion resistive metal, such as gold, tin, or nickel. Each patch can be designed with a variety of shapes, with the most popular shapes being rectangular or circular. The dielectric substrate is used primarily to provide proper spacing and mechanical support between the patch and its ground plane. It is also often used with high dielectric-constant material to load the patch and reduce its size. The substrate material should be low in insertion loss with a loss tangent of less than 0.005 [13], in particular for large array application. Generally, substrate materials can be separated into three categories in accordance with their dielectric constant [3]:

1. Having a relative dielectric constant $\varepsilon_r$ in the range of 1.0 to 2.0. This type of material can be air, polystyrene foam, or dielectric honeycomb.
2. Having $\varepsilon_r$ in the range of 2.0 to 4.0 with material consisting mostly of fiberglass reinforced Teflon.
3. With $\varepsilon_r$ between 4 and 10. The material can consist of ceramic, quartz, or alumina.

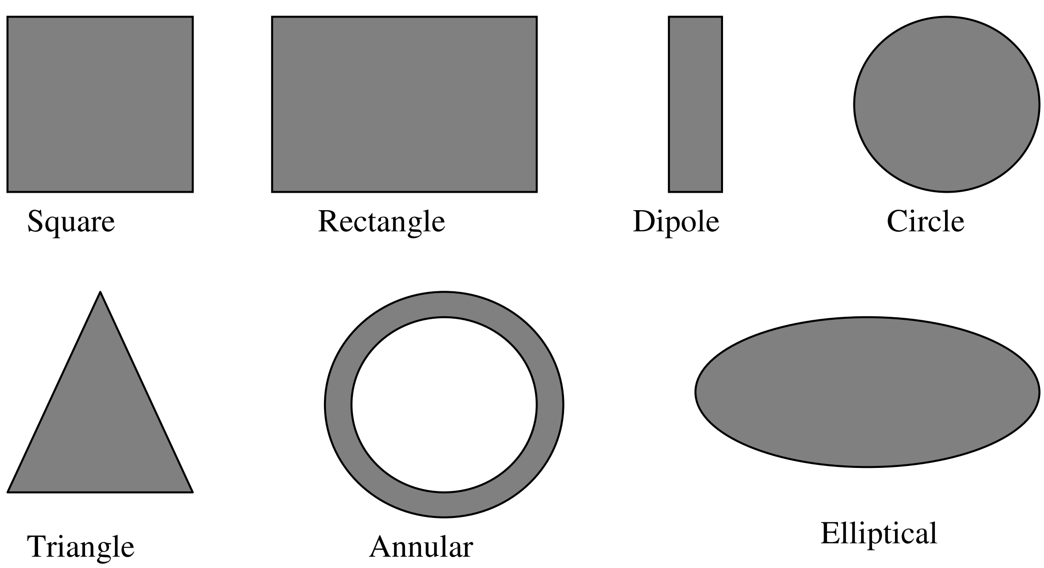


**Figure 2. 2 Geometry of commonly known microstrip patch antenna**

### 2.1.2 Advantages of Microstrip Antennas

Microstrip antennas have several advantages compared to conventional microwave antennas, and therefore many applications cover the broad frequency range from ~ 100 MHz to ~ 100 GHz. Some of the principal advantages of microstrip antennas compared to conventional microwave antennas are [13] and [3]:

- Light weight, low volume, low profile planar configurations, which can be made conformal.
- Low fabrication cost; readily amenable to mass production.
- Can be made thin hence they do not perturb the aerodynamics of host aerospace vehicles.
- The antennas may be easily mounted on missiles, rockets and satellites without major alterations.
- Linear, circular (left hand or right hand) polarizations are possible with simple modification of patch geometry and changes in feed position.
- Dual frequency antennas can be easily made.
- Microstrip antennas are compatible with modular designs (solid state devices such as oscillators, amplifiers, variable attenuators, switches, modulators, mixers, phase shifters etc., can be added directly to the antenna substrate board).
- Feed lines and matching networks are fabricated simultaneously with antenna structure.

### 2.1.3 Disadvantages of Microstrip Antennas

The microstrip antennas also have some disadvantages compared to conventional microwave antennas including [3]:

- Narrow bandwidth.
- Loss, hence somewhat lower gain.
- Practical limitations on the maximum gain $(\approx 20dB)$
- Poor end fire radiation performance
- Poor isolation between the feed and the radiating elements
- Possibility of excitation of surface waves
- Lower power handling capability

There are ways to minimize the effect of some of these limitations. For example, bandwidth can be increased to more than 60% by using special techniques; lower gain and lower power handling limitations can be over come thorough an array configuration. Surface wave associated limitations such as poor efficiency, increased mutual coupling, reduced gain and radiation pattern degradation can be over come by the use of photonic band gap structures.

### 2.1.4 Material Consideration

The purpose of the substrate material of a microstrip antenna is primarily to provide mechanical support for the radiating patch elements and to maintain the required precision spacing between the patch and its ground plane. With higher dielectric constant of the substrate material, the patch size can also be reduced due to loading effect. Certainly, with reduced antenna volume, higher dielectric constant also reduces bandwidth. There is a variety of types of substrate materials. As discussed in Section 2.1.1, the relative dielectric constant of these materials can be anywhere from 1 to 10 [3]. Materials with dielectric constants higher than 10 should be used with care. They can significantly reduce the radiation efficiency by having small antenna volumes. The most popular type of material is Teflon-based with a relative dielectric constant between 2 and 3. This Teflon-based material, also named PTFE (polytetrafluoroethylene), has a structure form very similar to the fiberglass material used for digital circuit boards, but it has a much lower loss tangent or insertion loss. The selection of the appropriate material for a microstrip antenna should be based on the desired patch size, bandwidth, insertion loss, thermal stability, cost, etc. For commercial application, cost is one of the most important criteria in determining the substrate type. For example, a single patch or an array of a few elements may be fabricated on a low-cost fiberglass material at the L-band frequency, while a 20-element array at 30 GHz may have to use higher-cost, but lower loss, Teflon-based material. For a large number of array elements at lower microwave frequencies (below 15 GHz), a dielectric honeycomb or foam panel may be used as substrate to minimize insertion loss, antenna mass, and material cost with increased bandwidth performance.

### 2.1.5 Applications of Microstrip Antennas

Notable system applications for which microstrip antennas have been developed include:

- Satellite communications
- Missile telemetry
- Man pack equipment
- Feed elements in complex antennas
- Satellite navigation receiver
- Biomedical radiator
- Command and control
- Direct broadcast satellite service
- Global positioning systems
- Medical Hyperthermia usage

## 2.2 Basic Principles of Operation

The metallic patch essentially creates a resonant cavity, where the patch is the top of the cavity, the ground plane is the bottom of the cavity, and the edges of the patch form the sides of the cavity. The edges of the patch act approximately as an open-circuit boundary condition. Hence, the patch acts approximately as a cavity with perfect electric conductor on the top and bottom surfaces, and a perfect "magnetic conductor" on the sides. This point of view is very useful in analyzing the patch antenna, as well as in understanding its behavior. Inside the patch cavity the electric field is essentially $z$ directed and independent of the z-coordinate [13]. Hence, the patch cavity modes are described by a double index ($m$, $n$). For the ($m$, $n$) cavity mode of the rectangular patch, the electric field has the form

$$E_z(x, y) = A_{mn} \cos\left(\frac{m\pi}{L} x\right)\cos\left(\frac{n\pi}{W} y\right) \qquad \text{(2.1)}$$

where $L$ is the patch length and $W$ is the patch width $A_{mn}$ is the modal wave amplitude, $n$ *and* $m$ are the mode numbers. The patch is usually operated in the (1, 0) mode, so that $L$ is the resonant dimension, and the field is essentially constant in the $y$ direction. The surface current $J_{sx}(x)$ on the bottom of the metal patch is then $x$ directed, and is given by

$$J_{sx}(x) = A_{10}\left(\frac{\pi / L}{j\omega\mu_0\mu_r}\right)\sin\left(\frac{\pi x}{L}\right) \qquad (2.2)$$

For this mode the patch may be regarded as a wide microstrip line of width *W*, having a resonant length *L* that is approximately one-half wavelength in the dielectric. The current is maximum at the center of the patch, $x = L/2$, while the electric field is maximum at the two "radiating" edges, $x = 0$ and $x = L$. The width *W* is usually chosen to be larger than the length ($W = 1.5\ L$ is typical) to maximize the bandwidth, since the bandwidth is proportional to the width. The width should be kept less than twice the length, however, to avoid excitation of higher order modes.

At first glance, it might appear that the microstrip antenna will not be an effective radiator when the substrate is thin, since the patch current will be effectively shorted by the close proximity to the ground plane. If the modal amplitude $A_{10}$ were constant, the strength of the radiated field would in fact be proportional to *h*. However, the Q of the cavity increases as *h* decreases (the radiation Q is inversely proportional to *h*). Hence, the amplitude $A_{10}$ of the modal field at resonance is inversely proportional to *h*. Hence, the strength of the radiated field from a resonant patch is essentially independent of *h*, if losses are ignored. The resonant input resistance will likewise be nearly independent of *h*. This explains why a patch antenna can be an effective radiator even for very thin substrates, although the bandwidth will be small.

## 2.3 Feeding Techniques

The microstrip antenna may be fed in various ways.

### 2.3.1 Coaxial probe feed

Perhaps the most common type of feeding techniques is the direct probe feed, shown in Figure 2.3 for a rectangular patch, where the center conductor of a coaxial feed line penetrates the substrate to make direct contact with the patch. For linear polarization, the patch is usually fed along the centerline, $y = W/2$ [1]. The feed point location at $x = x_f$ controls the resonant input resistance. The input resistance is highest when the patch is fed at the edge, and smallest (essentially zero) when the patch is fed at the center ($x = L/2$).

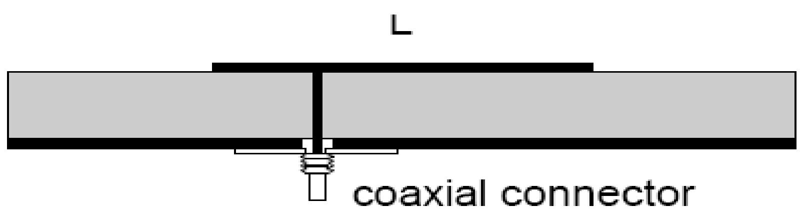


**Figure 2. 3 Probe fed microstrip patch antenna**

### 2.3.2 Microstrip feed line

Another common feeding technique, preferred for planar fabrication, is the direct-contact microstrip feed line, shown in Figure 2.4. An inset notch is used to control the resonant input resistance at the contact point. The input impedance seen by the microstrip line is approximately the same as that seen by a probe at the contact point, provided the notch does not disturb the modal field significantly [13].

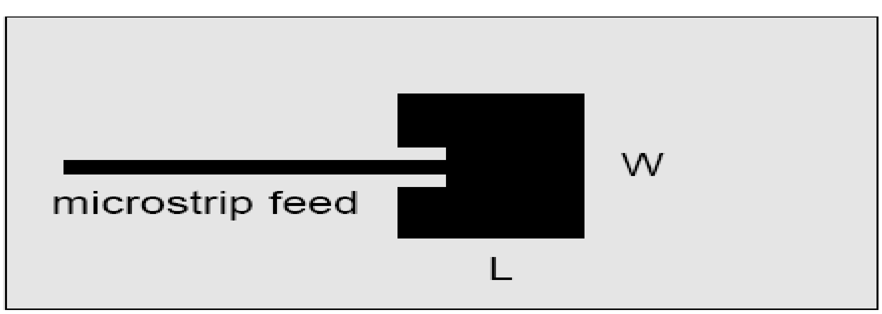


**Figure 2. 4 Direct contact microstrip feed line**

### 2.3.3 Aperture coupling

Aperture Coupling is another type of EMC feed. Pozar [12] first proposed this type of feed to increase the bandwidth of the MSA. The RF energy from the feed line is coupled to the radiating element through a common aperture in the form of a rectangular slot. It mainly consists of two substrates separated by a ground plane. Top substrate is for the radiating element and the bottom substrate is for the feed-line. A slot is made in the ground plane to provide coupling between the feed line and patch.

For the sake of maximum coupling the slot is usually placed at the center and it is perpendicular to the feed line, as a result the patch and the slot may share common center. The length of the slot should be kept some how larger than the width of the slot. The diagrammatic setup for aperture coupling is shown below.

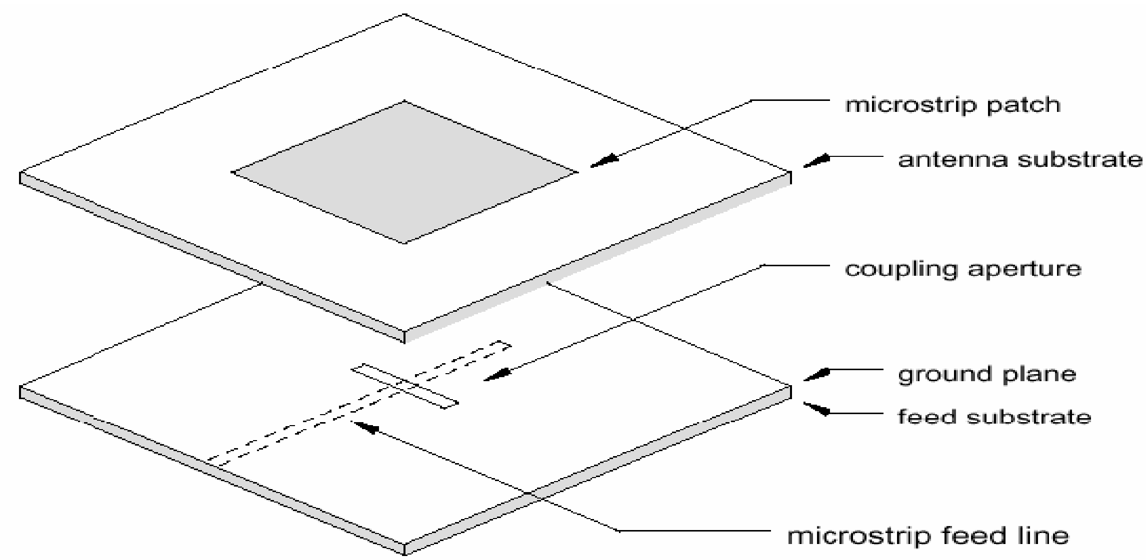


**Figure 2. 5 Aperture coupled Microstrip patch antenna**

This scheme has the advantage of isolating the feeding network from the radiating patch element. It also overcomes the limitation on substrate thickness imposed by the feed inductance of a coaxial probe, so that thicker substrates and hence higher bandwidths can be obtained but it suffers from high back radiation.

### 2.3.4 Proximity coupled feed

Proximity coupling [1] is a type of EMC feed, this has many advantages over edge fed and coaxial fed antenna. Proximity-coupled microstrip antenna is also known as non-contacting feeds. Some advantages are:

- No physical contact between feed line and radiating element.
- No drilling required.
- Less spurious radiation.
- Better for array configurations.
- Good suppression of higher order modes
- Better high frequency performance

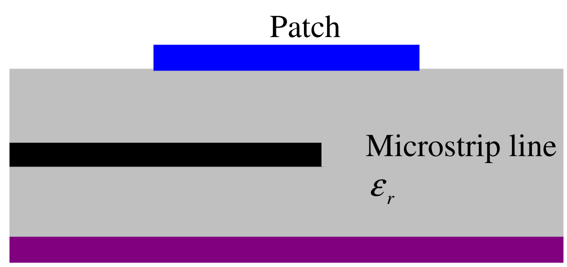


**Figure 2. 6 Proximity coupled patch**

Matching can be achieved by controlling the length of the feed line and the width-to-line ratio of the patch. The major disadvantage of this feed scheme is that it is difficult to fabricate because of the two dielectric layers which need proper alignment. Also, there is an increase in the overall thickness of the antenna.

## 2.4 Methods of Analysis

The most popular models for the analysis of Microstrip patch antennas are the transmission line model, cavity model, and full wave model (which include primarily integral equations/Moment Method) [1]. The transmission line model is the simplest of all and it gives good physical insight but it is less accurate. The cavity model is more accurate and gives good physical insight but is complex in nature. The full wave models are extremely accurate, versatile and can treat single elements, finite and infinite arrays, stacked elements, arbitrary shaped elements and coupling. These give less insight as compared to the two models mentioned above and are far more complex in nature.

### 2.4.1 Transmission Line Model

This model represents the microstrip antenna by two slots of width *W* and height *h,* separated by a transmission line of length L. The microstrip is essentially a non-homogeneous line of two dielectrics, typically the substrate and air.

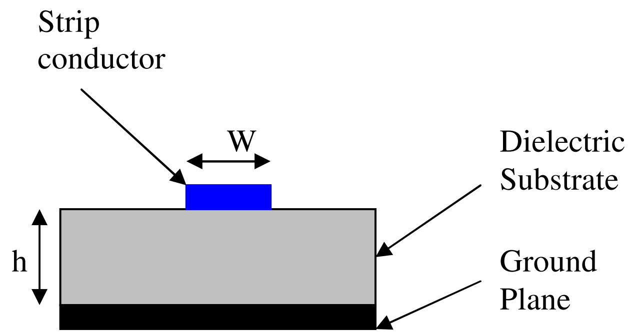


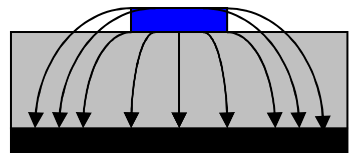

**Figure 2. 7 Microstrip Line** **Figure 2. 8 Electric Field Lines**

Hence, as seen from Figure 2.8, most of the electric field lines reside in the substrate and parts of some lines in air. As a result, this transmission line cannot support pure transverse electro-magnetic (TEM) mode of transmission, since the phase velocities would be different in the air and the substrate. Instead, the dominant mode of propagation would be the quasi-TEM mode. Hence, an effective dielectric constant ($\varepsilon_{reff}$) must be obtained in order to account for the fringing and the wave propagation in the line. The value of $\varepsilon_{reff}$ is slightly less than $\varepsilon_r$ because the fringing fields around the periphery of the patch are not confined in the dielectric substrate but are also spread in the air as shown in Figure 2.8 above. The expression for $\varepsilon_{reff}$ is given as [1]:

$$\varepsilon_{reff} = \frac{\varepsilon_r + 1}{2} + \frac{\varepsilon_r - 1}{2}\left[1 + 12\frac{h}{W}\right]^{-\frac{1}{2}} \quad (2.3)$$

Where $\varepsilon_{reff}$ = Effective dielectric constant

$\varepsilon_r$ = Dielectric constant of substrate

$h$ = Height of dielectric substrate

$W$ = Width of the patch

Consider Figure 2.9 below, which shows a rectangular microstrip patch antenna of length *L,* width *W* resting on a substrate of height *h.* The co-ordinate axis is selected such that the length is along the *x* direction, width is along the *y* direction and the height is along the *z* direction.

In order to operate in the fundamental $TM_{10}$ mode, the length of the patch must be slightly less than $\lambda/2$ where $\lambda$ is the wavelength in the dielectric medium and is equal to

$\lambda_0 / \sqrt{\varepsilon_{reff}}$ where $\lambda_0$ is the free space wavelength. The $TM_{10}$ mode implies that the field varies one $\lambda/2$ cycle along the length, and there is no variation along the width of the patch. In the Figure 2.9 shown below, the microstrip patch antenna is represented by two slots, separated by a transmission line of length L and open circuited at both the ends. Along the width of the patch, voltage is maximum and current is minimum due to the open ends.

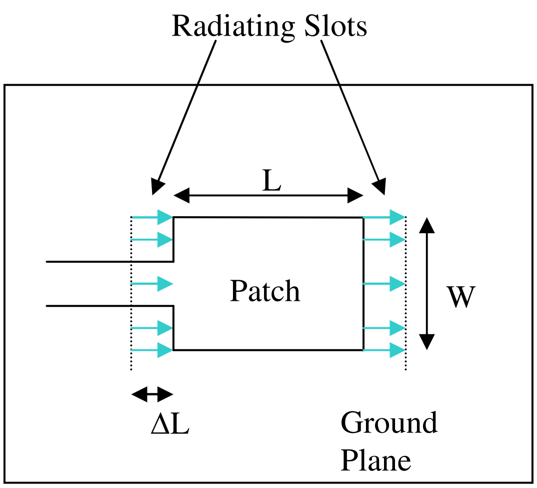


**Figure 2. 9 Top view of a patch antenna**

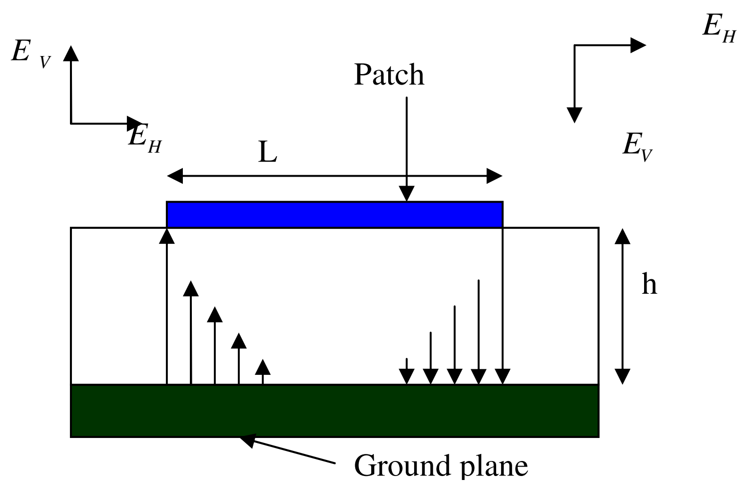


**Figure 2. 10 Side view of the patch antenna**

It is seen from Figure 2.10 that the normal components of the electric field at the two edges along the width are in opposite directions and thus out of phase since the patch is $\lambda/2$ long and hence they cancel each other in the broadside direction. The tangential components (seen in Figure 2.10), which are in phase, means that the resulting fields combine to give maximum radiated field normal to the surface of the structure. Hence the edges along the width can be represented as two radiating slots, which are $\lambda/2$ apart and excited in phase and radiating in the half space above the ground plane. The fringing fields along the width can be modeled as radiating slots and electrically the patch of the microstrip antenna looks greater than its physical dimensions. The dimensions of the patch along its length have now been extended on each end by a length $\Delta L$, which is given empirically by Hammerstad formula [1] as:

$$\Delta L = 0.412h \frac{\left(\varepsilon_{reff} + 0.3\right)\left(\frac{W}{h} + 0.264\right)}{\left(\varepsilon_{reff} - 0.258\right)\left(\frac{W}{h} + 0.8\right)} \quad \ldots\ldots\ldots\ldots\ldots\ldots\ldots\ldots\ldots\ldots\ldots \text{(2.4)}$$

The effective length of the patch $L_{eff}$ now becomes:

$$L_{eff} = L + 2\Delta L \quad \ldots\ldots\ldots\ldots\ldots\ldots\ldots\ldots\ldots\ldots\ldots\ldots\ldots\ldots\ldots\ldots\ldots \text{(2.5)}$$

For a given resonance frequency $f_0$ for the (1, 0) mode, the effective length is given by:

$$L_{eff} = \frac{c}{2 f_0 \sqrt{\varepsilon_{reff}}} \quad \ldots\ldots\ldots\ldots\ldots\ldots\ldots\ldots\ldots\ldots\ldots\ldots\ldots\ldots\ldots\ldots \text{(2.6)}$$

$$W = \frac{c}{2 f_0 \sqrt{\frac{\varepsilon_r + 1}{2}}} \quad \ldots\ldots\ldots\ldots\ldots\ldots\ldots\ldots\ldots\ldots\ldots\ldots\ldots\ldots\ldots\ldots \text{(2.7)}$$

For a rectangular Microstrip patch antenna, the resonance frequency for any $TM_{mn}$ mode is given as [8]:

$$f_0 = \frac{c}{2\sqrt{\varepsilon_{reff}}} \left[ \left(\frac{m}{L}\right)^2 + \left(\frac{n}{W}\right)^2 \right]^{\frac{1}{2}} \quad \ldots\ldots\ldots\ldots\ldots\ldots\ldots\ldots\ldots\ldots\ldots\ldots \text{(2.8)}$$

where m and n are modes along $L$ and $W$ respectively.

### 2.4.2 Cavity Model

Although the transmission line model discussed in the previous section is easy to use, it has some inherent disadvantages. Specifically, it is useful for patches of rectangular design and it ignores field variations along the radiating edges. These disadvantages can be overcome by using the cavity model. A brief overview of this model is given below. In this model, the interior region of the dielectric substrate is modeled as a cavity bounded by electric walls on the top and bottom. The magnetic cavity model works best for thin substrates $(h << \lambda)$. In this case the TM modes are superior in the cavity. The cavity model makes the following assumptions:

- The electric field is *z*-directed, and the magnetic field has only a transverse components $H_x$ and $H_y$ in the cavity (the region bounded by the patch metallization and the ground plane).

- Since the substrate is assumed thin, the fields in the cavity do not vary with $z$
- The tangential component of the magnetic field is negligible at the edge of the patch
- The existence of a fringing field can be accounted for by slightly extending the edges of the patch.

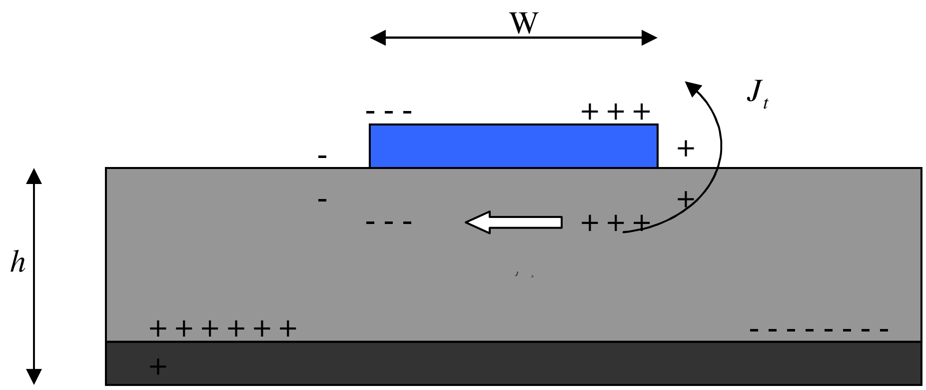


**Figure 2. 11 Charge distribution and current density creation on a microstrip patch antenna**

Consider Figure 2.11 shown above. When the microstrip patch is provided power, a charge distribution is seen on the upper and lower surfaces of the patch and at the bottom of the ground plane. This charge distribution is controlled by two mechanisms-an attractive mechanism and a repulsive mechanism. The attractive mechanism is between the opposite charges on the bottom side of the patch and the ground plane, which helps in keeping the charge concentration intact at the bottom of the patch. The repulsive mechanism is between the like charges on the bottom surface of the patch, which causes pushing of some charges from the bottom to the top of the patch [1]. As a result of this charge movement, currents flow at the top and bottom surface of the patch. The cavity model assumes that the height to width ratio (i.e. height of substrate and width of the patch) is very small and as a result the attractive mechanism dominates and causes most of the charge concentration and the current to be below the patch surface. Much less current would flow on the top surface of the patch and as the height to width ratio further decreases, the current on the top surface of the patch would be almost equal to zero, which would not allow the creation of any tangential magnetic field components to the patch edges. Hence, the four sidewalls could be modeled as perfectly magnetic conducting surfaces. This implies that the magnetic fields and the electric field distribution beneath the patch would not be disturbed. However, in practice, a finite width to height ratio would be there and this would not make the tangential magnetic fields to be completely zero, but they being very small, the side walls could be approximated to be perfectly magnetic conducting.

Since the walls of the cavity, as well as the material within it are lossless, the cavity would not radiate and its input impedance would be purely reactive. Hence, in order to account for radiation and a loss mechanism, one must introduce a radiation resistance $R_r$ and a loss resistance $R_L$. A lossy cavity would now represent an antenna and the loss is taken into account by the effective loss tangent $\delta_{eff}$ which is given as:

$$\delta_{eff} = \frac{1}{Q_T} \quad \text{......} \quad (2.9)$$

$Q_T$ is the total antenna quality factor and is expressed in the form:

$$\frac{1}{Q_T} = \frac{1}{Q_c} + \frac{1}{Q_d} + \frac{1}{Q_r} \quad \text{......} \quad (2.10)$$

- $Q_c$ represents the quality factor of the conductor and is given by:

$$Q_c = \frac{\omega_r W_T}{P_c} = \frac{h}{\Delta} \quad \text{......} \quad (2.11)$$

where $P_c$ is the conductor loss

$\Delta$ is the skin depth of the conductor

$h$ is the height of the substrate

$W_T$ is the total energy stored in the patch at resonance

- $Q_d$ represents the quality factor of the dielectric and is given by:

$$Q_d = \frac{\omega_r W_T}{P_d} = \frac{1}{\tan\delta} \quad \text{......} \quad (2.12)$$

where $\omega_r$ is the angular resonant frequency

$P_d$ is the dielectric loss

$\tan\delta$ is the loss tangent of the dielectric

- $Q_r$ represents the quality factor for radiation and is given as:

$$Q_r = \frac{\omega_r W_T}{P_r} \quad \ldots\ldots (2.13)$$

where $P_r$ is the power radiated from the patch.

Substituting the three equations obtained above, we get

$$\delta_{eff} = \tan\delta + \frac{\Delta}{h} + \frac{P_r}{\omega_r W_T} \quad \ldots\ldots (2.14)$$

This equation describes the effective loss tangent of a microstrip patch antenna.

## 2.5 Radiation Patterns of a Microstrip Patch Antenna

The radiation field of the microstrip antenna may be determined using either an "electric current" model or a "magnetic current" model. In the electric current model, the current is used directly to find the far-field radiation pattern. If the substrate is neglected (replaced by air) for the calculation of the radiation pattern, the pattern may be found directly from image theory. If the substrate is accounted for, and is assumed infinite, the reciprocity method may be used to determine the far-field pattern.

In the magnetic current model, the equivalence principle [14] is used to replace the patch by a magnetic surface current that flows on the perimeter of the patch. The magnetic surface current is given by [13]

$$M_s = -\hat{n} \times E \quad \ldots\ldots (2.15)$$

where $E$ is the electric field of the cavity mode at the edge of the patch and $\hat{n}$ is the outward pointing unit-normal vector at the patch boundary. The far-field pattern may once again be determined by image theory or reciprocity, depending on whether the substrate is neglected or not. The dominant part of the radiation field comes from the "radiating edges" at $x = 0$ and $x = L$. The two non-radiating edges do not affect the pattern in the principle planes (the E plane at $\phi = 0$ and the H plane at $\phi = \pi/2$), and have a small effect for other planes [1].

It can be shown that the electric and magnetic current models yield exactly the same result for the far-field pattern, provided the pattern of each current is calculated in the presence of the substrate at the resonant frequency of the patch cavity mode [5]. If the substrate is neglected, the agreement is only approximate, with the largest difference being near the horizon.

According to the electric current model, accounting for the infinite substrate the far field is given [13] by,

$$E_i(r,\theta,\phi) = E_i^h(r,\theta,\phi)\left(\frac{\pi WL}{2}\right)\left[\frac{\sin\left(\frac{k_y W}{2}\right)}{\frac{k_y W}{2}}\right]\left[\frac{\cos\left(\frac{k_x L}{2}\right)}{\left(\frac{\pi}{2}\right)^2 - \left(\frac{k_x L}{2}\right)^2}\right] \quad \ldots\ldots\ldots\ldots\ldots\ldots\ldots \text{(2.16)}$$

where $k_x = k_0 \sin\theta \, \cos\phi$

$k_y = k_0 \sin\theta \, \cos\phi$

and $E_i^h$ is the far-field pattern of an infinitesimal (Hertzian) unit-amplitude *x*-directed electric dipole at the center of the patch. This pattern is given by [13]

$$E_\theta^h(r,\theta,\phi) = E_0 \cos\phi \; G(\theta) \ldots\ldots\ldots\ldots\ldots\ldots\ldots\ldots\ldots\ldots\ldots\ldots\ldots\ldots \text{(2.17)}$$

$$E_\phi^h(r,\theta,\phi) = -E_0 \sin\phi \; F(\theta) \ldots\ldots\ldots\ldots\ldots\ldots\ldots\ldots\ldots\ldots\ldots\ldots\ldots\ldots \text{(2.18)}$$

where
$$E_0 = \left(\frac{-j\omega\mu_0}{4\pi r}\right) e^{-jk_0 r} \ldots\ldots\ldots\ldots\ldots\ldots\ldots\ldots\ldots\ldots\ldots\ldots\ldots \text{(2.19)}$$

$$F(\theta) = \frac{2\tan\left(k_0 h N(\theta)\right)}{\tan\left(k_0 h N(\theta)\right) - j\dfrac{N(\theta)}{\mu_r}\sec\theta} \ldots\ldots\ldots\ldots\ldots\ldots\ldots\ldots\ldots\ldots\ldots\ldots\ldots \text{(2.20)}$$

$$G(\theta) = \frac{2\tan\left(k_0 h N(\theta)\right)\cos\theta}{\tan\left(k_0 h N(\theta)\right) - j\dfrac{\varepsilon_r}{N(\theta)}\cos\theta} \ldots\ldots\ldots\ldots\ldots\ldots\ldots\ldots\ldots\ldots\ldots\ldots\ldots \text{(2.21)}$$

and

$$N(\theta) = \sqrt{n_1^2 - \sin^2(\theta)} \ldots\ldots\ldots\ldots\ldots\ldots\ldots\ldots\ldots\ldots\ldots\ldots\ldots\ldots\ldots\ldots \text{(2.22.)}$$

$$n_1 = \sqrt{\varepsilon_r \mu_r} \ldots\ldots\ldots\ldots\ldots\ldots\ldots\ldots\ldots\ldots\ldots\ldots\ldots\ldots\ldots\ldots\ldots\ldots\ldots \text{(2.23)}$$

## 2.6 Radiation Efficiency of Microstrip Patch

The radiation efficiency of the patch antenna is affected not only by conductor and dielectric losses, but also by surface-wave excitation -- since the dominant $TM_{10}$ mode of the grounded substrate will be excited by the patch. As the substrate thickness decreases, the effect of the conductor and dielectric losses becomes more severe, limiting the efficiency. On the other hand, as the substrate thickness increases, the surface-wave power increases, thus limiting the efficiency. Surface-wave excitation is undesirable for other reasons as well, since surface waves contribute to mutual coupling between elements in an array, and also cause undesirable edge diffraction at the edges of the ground plane or substrate, which often contributes to distortions in the pattern and to back radiation. For an air (or foam) substrate there is no surface-wave excitation. In this case, higher efficiency is obtained by making the substrate thicker, to minimize conductor and dielectric losses (making the substrate too thick may lead to difficulty in matching, however, as discussed above). For a substrate with a moderate relative permittivity such as $\varepsilon_r = 2.2$, the efficiency will be maximum when the substrate thickness is approximately $0.02\lambda_0$ [1].

The radiation efficiency is defined as [1] and [13]

$$e_r = \frac{P_{sp}}{P_{total}} = \frac{P_{sp}}{P_{sp} + P_c + P_d + P_{sw}} \quad \text{.......} \quad (2.24)$$

Where $P_{sp}$ is the power radiated into space, and the total input power $P_{total}$ is given as the sum of $P_c$ -- the power dissipated by conductor loss, $P_d$ -- the power dissipated by dielectric loss, and $P_{sw}$ -- the surface-wave power. The efficiency may also be expressed in terms of the corresponding Q factors as

$$e_r = \frac{Q_{total}}{Q_{sp}} \quad \text{.......} \quad (2.25)$$

$$\frac{1}{Q_{total}} = \frac{1}{Q_{sp}} + \frac{1}{Q_{sw}} + \frac{1}{Q_d} + \frac{1}{Q_c} \quad \text{.......} \quad (2.26)$$

The dielectric and conductor Q factors are given by

$$Q_d = \frac{1}{\tan\delta} \quad \text{.......} \quad (2.27)$$

$$Q_c = \frac{1}{2}\eta_0\mu_r\left(\frac{k_0 h}{R_s}\right) \quad \text{……………………………………………………} (2.28)$$

where $\tan\delta$ is the loss tangent of the substrate and $R_s$ is the surface resistance of the patch and ground plane metal at radian frequency $\omega = 2\pi f$ , given by

$R_s = \sqrt{\frac{\omega\mu_0}{2\sigma}}$ , where $\sigma$ is the conductivity of the metal.

The space-wave Q factor is given approximately as [13]

$$Q_{sp} = \frac{3}{16}\left(\frac{\varepsilon_r}{pc_1}\right)\left(\frac{L}{W}\right)\left(\frac{1}{h/\lambda_0}\right) \quad \text{……………………………………………………} (2.29)$$

$$c_1 = 1 - \frac{1}{n_1^2} + \frac{2/5}{n_1^4} \quad \text{……………………………………………………} (2.30)$$

$$p = 1 + \frac{a_2}{10}(k_0W)^2 + \left(a_2^2 + 2a_4\right)\left(\frac{3}{560}\right)(k_0W)^4 + c_2\left(\frac{1}{5}\right)(k_0L)^2 + a_2c_2\left(\frac{1}{70}\right)(k_0W)^2(k_0L)^2,$$

with $a_2 = -0.16605,\ a_4 = 0.00761,\ and\ c_2 = -0.0914153.$

The surface-wave Q factor is related to the space-wave Q factor as [13]

$$Q_{sw} = Q_{sp}\left(\frac{e_r^{sw}}{1 - e_r^{sw}}\right), \quad \text{……………………………………………} (2.31)$$

where $e_r^{sw}$ is the radiation efficiency accounting only for surface-wave loss. This efficiency may be accurately approximated by using the radiation efficiency of an infinitesimal dipole on the substrate layer [13], giving

$$e_r^{sw} = \frac{1}{1 + (k_0h)\left(\frac{3}{4}\right)(\pi\mu_r)\left(\frac{1}{c_1}\right)\left(1 - \frac{1}{n_1^2}\right)^3} \quad \text{………………………………} (2.32)$$

## 2.7 Bandwidth of a Microstrip Patch

The bandwidth increases as the substrate thickness increases (the bandwidth is directly proportional to $h$ if conductor, dielectric, and surface-wave losses are ignored). However, increasing the substrate thickness lowers the $Q$ of the cavity, which increases spurious radiation from the feed, as well as from higher-order modes in the patch cavity. Also, the patch typically becomes difficult to match as the substrate thickness increases beyond a certain point (typically about $0.05\lambda_0$). This is especially true when feeding with a coaxial probe, since a thicker substrate results in a larger probe inductance appearing in series with the patch impedance. However, in recent years considerable effort has been spent to improve the bandwidth of the microstrip antenna, in part by using alternative feeding schemes. The aperture-coupled feed of Figure 2.5 is one scheme that overcomes the problem of probe inductance, at the cost of increased complexity.

Lowering the substrate permittivity also increases the bandwidth of the patch antenna. However, this has the disadvantage of making the patch larger. Also, because the $Q$ of the patch cavity is lowered, there will usually be increased radiation from higher-order modes, degrading the polarization purity of the radiation.

A CAD formula for the bandwidth (defined by $VSWR \leq 2$) is [13]

$$BW = \frac{1}{\sqrt{2}}\left[\tan\delta + \left(\frac{R_s}{\pi\eta_0\mu_r}\right)\left(\frac{1}{h/\lambda_0}\right) + \left(\frac{16}{3}\right)\left(\frac{pc_1}{\varepsilon_r}\right)\left(\frac{h}{\lambda_0}\right)\left(\frac{W}{L}\right)\left(\frac{1}{e_r^{sw}}\right)\right] \quad \text{............(2.33)}$$

where the terms have been defined in the previous section on radiation efficiency. The result should be multiplied by 100 to get percent bandwidth. Note that neglecting conductor and dielectric loss yields a bandwidth that is directly proportional to the substrate thickness $h$.

# Chapter 3

## Microstrip Patch Antenna Design Techniques

The procedure for designing a rectangular microstrip patch antenna is explained in this section. To demonstrate the procedure, a compact rectangular microstrip patch antenna is designed for use in the wireless local area network (WLAN).

The main factors involved in the design of a single patch antenna are [3];

- Selection of substrate material
- Feed position & its location
- Patch dimensions.

For the selection of substrate, the major electrical properties to consider are relative dielectric constant and loss tangent. The selection of substrate material plays a very important role in patch antenna design. A higher loss tangent reduces antenna efficiency and increases feed losses. A higher dielectric constant results in smaller patch but generally reduces bandwidth resulting in tighter fabrication tolerance. The substrate thickness should be chosen as large as possible to maximize bandwidth and efficiency, but not so large to risk surface wave excitation.

Approximate performance trade-offs for a rectangular patch are summarized below [3];

| Requirement | Substrate height | Substrate relative permittivity | Patch width |
|---|---|---|---|
| High radiation efficiency | thick | low | wide |
| Low dielectric loss | thin | low | -- |
| Low conductor loss | thick | -- | -- |
| Wide (impedance) bandwidth | thick | low | wide |
| Low extraneous (surface wave) radiation | thin | low | -- |
| Low cross polarization | -- | low | -- |
| Light weight | thin | low | -- |
| Strong | thick | high | -- |
| Low sensitivity tolerances | thick | low | wide |

## Design Specifications

The three essential parameters for the design of a rectangular Microstrip Patch Antenna are [3]:

- Frequency of operation $(f_0)$: The resonant frequency of the antenna must be selected appropriately. The wireless local area network (WLAN) used in this thesis work operates in the frequency range from 3-4.2 GHz. Hence the antenna designed must be able to operate in this frequency range. The resonant frequency selected in this case is 3.5 GHz.
- Dielectric constant of the substrate $(\varepsilon_r)$: The dielectric material selected in this thesis is Rogers RT 5880 which has a dielectric constant of 2.2. The dielectric constant is kept low to get better bandwidth. The choice of high dielectric substrate results in size reduction at the expense of bandwidth reduction.
- Height of dielectric substrate $(h)$: For the microstrip patch antenna to be used in the aforementioned frequency range, the antenna size may be moderate in thickness. In this design, the height of the dielectric substrate is selected is 1.6 mm.

The design procedure used throughout this thesis is applicable for antennas that work in the frequency range of 3.0-4.2GHz. The frequency band is used in digital audio radio satellite(DARS), direct-to-home satellite television, mobile satellite services, network equipment compatible with IEEE 802.11b and 802.11g, 802.16a and 802.16e IEEE 802.11a WIFI and cordless phone applications etc. The design techniques are also applicable to any frequency ranges, which can be selected according to the designer's wish.

Hence, the essential parameters for the design are: $f_0 = 3.5GHz$, $\varepsilon_r = 2.2$, and $h = 1.6mm$. Usually the thickness of the dielectric substrate is in the range $0.003\lambda_0 \le h \le 0.05\lambda_0$ and the length of the patch is $0.30\lambda_0 < L < 0.5\lambda_0$, where $\lambda_0$ is the free space wavelength. If the thickness is greater than $0.05\lambda_0$ the feed probe inductance becomes severe which might cause matching difficult even though the impedance bandwidth shows an increase. The transmission line model described in chapter 3 is used to design the antenna.

The Design Procedures

**Step 1: Width Calculation** $(W)$: the width of a microstrip patch is given by equation (2.7)

$$W = \frac{c}{2f_0\sqrt{\frac{\varepsilon_r + 1}{2}}}$$

$c = 3\times10^8 m/s$, $f_0 = 3.50 GHz$ $\varepsilon_{reff} = 2.2$ gives $W = 34.0mm$

**Step 2: Calculation of Effective dielectric constant** $(\varepsilon_{reff})$**:** The effective dielectric constant is given by equation (2.3):

$$\varepsilon_{reff} = \frac{\varepsilon_r + 1}{2} + \frac{\varepsilon_r - 1}{2}\left[1 + 12\frac{h}{W}\right]^{-\frac{1}{2}}$$

Substituting $\varepsilon_{reff} = 2.2$, $W = 34.0mm$ and $h = 1.6mm$ we get: $\varepsilon_{reff} = 2.11$

**Step 2: Calculation of the Effective length** $(L_{eff})$**:** Equation (2.6) gives the effective length as [3]: $L_{eff} = \dfrac{c}{2f_0\sqrt{\varepsilon_{reff}}}$

Substituting $\varepsilon_{reff} = 2.108$, $c = 3\times10^8 m/s$ and $f_0 = 3.50 GHz$ we get:

$L_{eff} = 0.0344m = 34.4mm$.

**Step 3: Calculation of the length extension (**$\Delta L$**):** Equation (2.4) gives the length extension as: $W/h = 21.25$

$$\Delta L = 0.412h\frac{(\varepsilon_{reff} + 0.3)\left(\frac{W}{h} + 0.264\right)}{(\varepsilon_{reff} - 0.258)\left(\frac{W}{h} + 0.8\right)}$$

Substituting $\varepsilon_{reff} = 2.11$, $W = 34.0mm$ and $h = 1.6mm$ we get: $\Delta L = 0.840mm$

**Step 4: Calculation of actual length of patch** $(L)$**:** The actual length is obtained by re-writing equation (2.5) as:

$$L = L_{eff} - 2\Delta L$$

Substituting $L_{eff} = 34.4mm$ and $L = 27mm$.

The width to length ratio of the patch is 1.26, sometimes known as aspect ratio of the patch. Typically the width of patch is taken to be $W \leq 2L$ [1] for wideband design. In this case $W = 1.5L$ is used in my design.

**Step 5: Determination of Feed point Location:**

A coaxial probe type feed is to be used in this design. The feed point must be located at that point on the patch, where the input impedance is 50 ohms for the resonant frequency. Hence, a trial and error method is used to locate the feed point. For different locations of the feed point, the return loss (R.L) is compared and that feed point is selected where the R.L is most negative.

The performance of the designed antenna is studied using the Sonnet Software package and the following results are obtained.

(a) Return Loss Curve

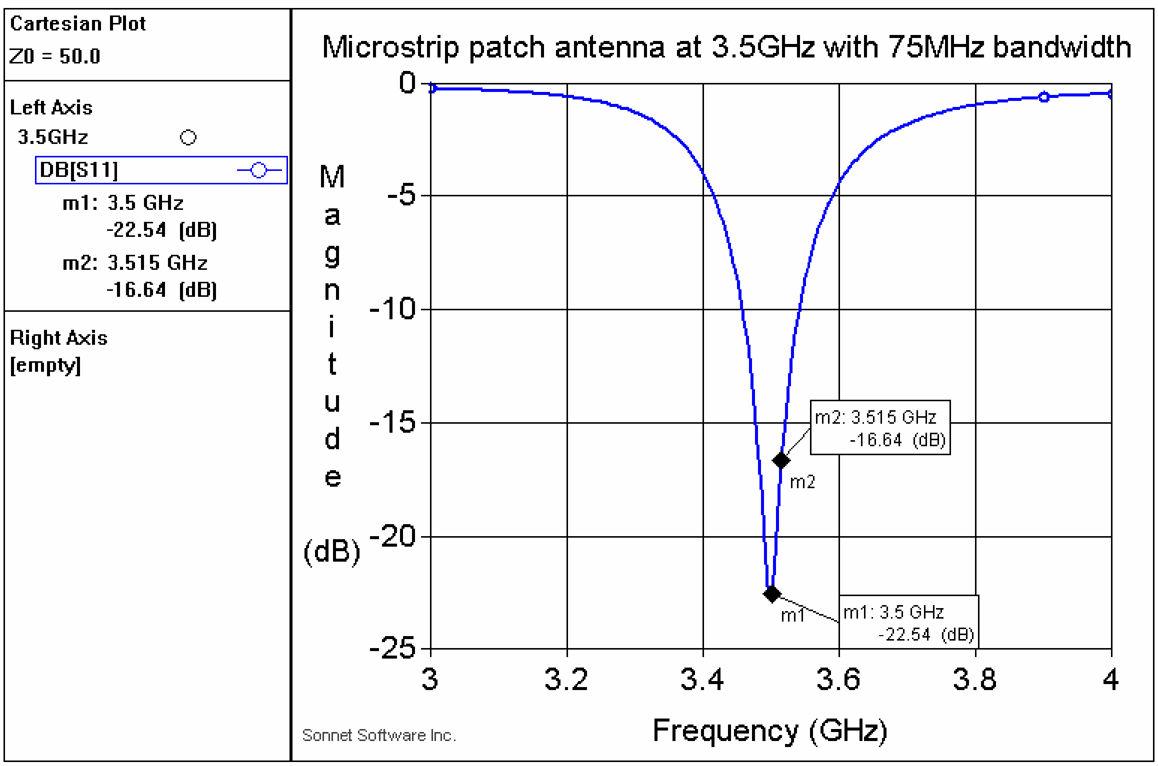


**Figure 3. 1 Return loss obtained in the above design**

The graph shows a plot of the reflection coefficient (S11) in decibel versus frequency. The antenna has a bandwidth of 75MHz. It has 2.29% bandwidth of the operating frequency 3.5GHz.

(b) Input Impedance Curve

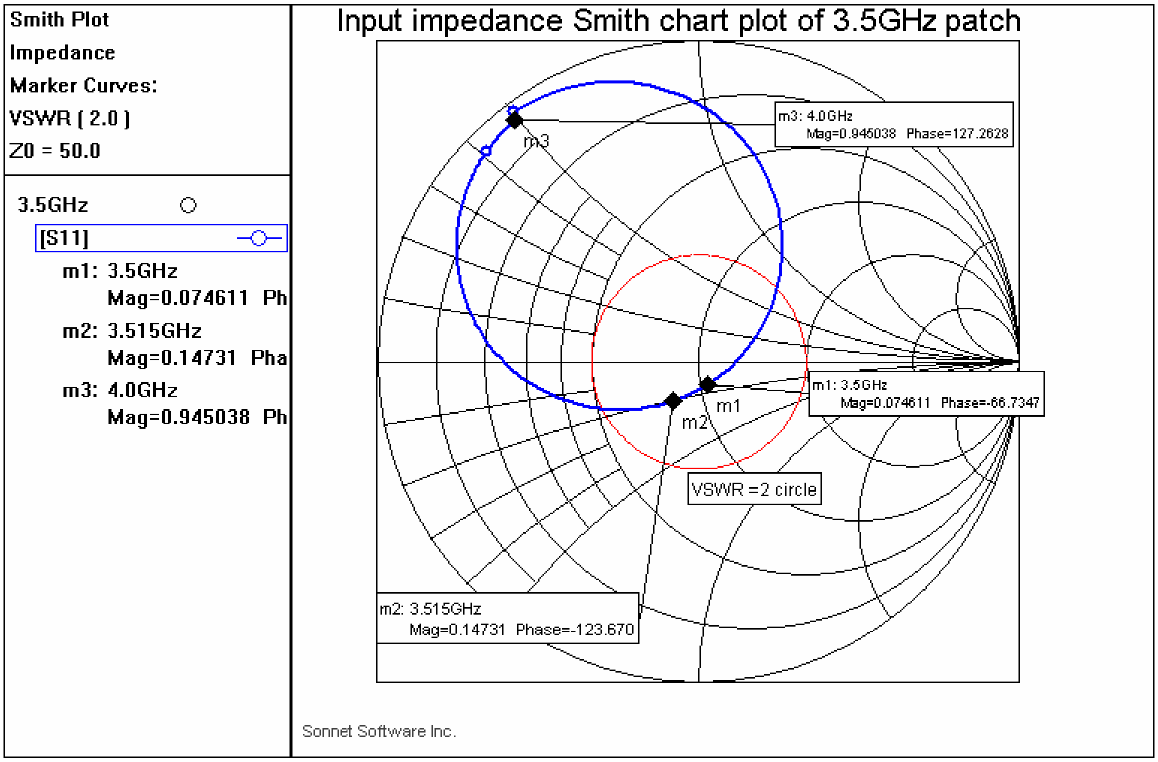


**Figure 3. 2 The impedance curve on the Smith chart**

The above graph shows the input impedance curve on a Smith Chart. The red circle is a curve showing VSWR=2. The blue one is the input impedance curve of the antenna under consideration. The points on the curve are the magnitude and phase of the normalized (with respect to 50 ohms) impedance at the corresponding frequency.

(c) Radiation Pattern Plot

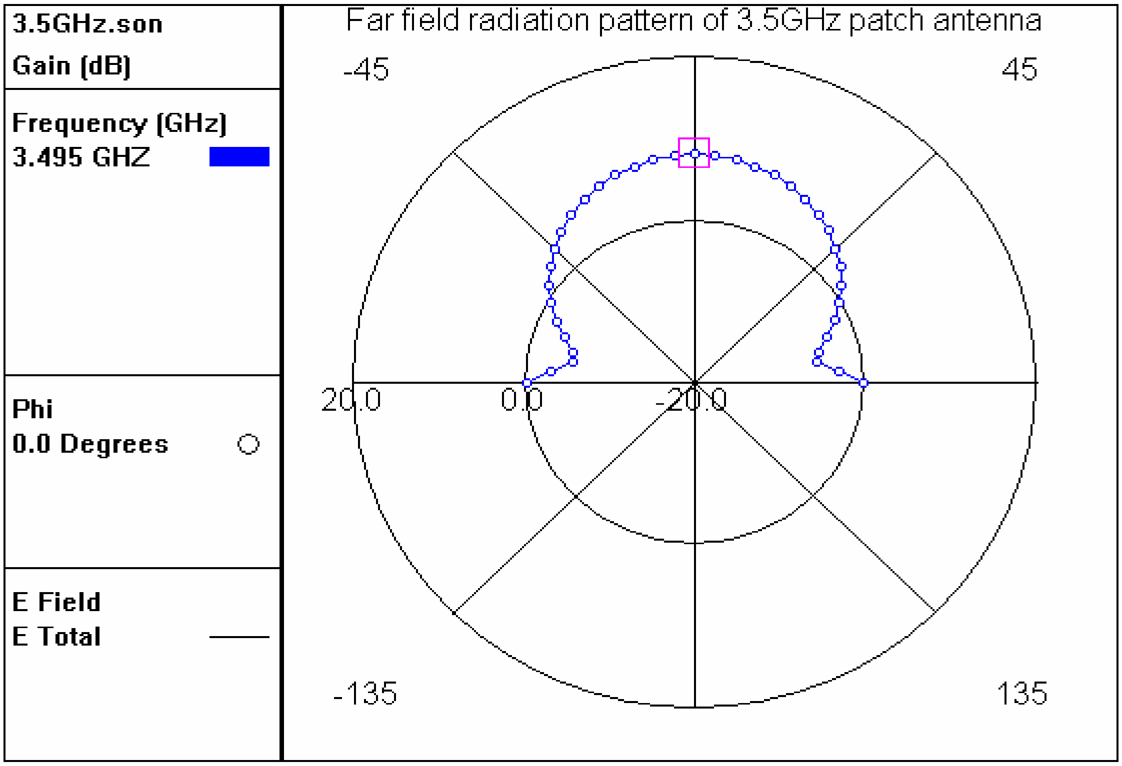


**Figure 3. 3 The radiation pattern the conventional patch antenna**

This figure shows the radiation pattern of the 3.5 GHz patch antenna. From the graph we observe that the gain is about 8.044dBi at 3.495GHz for theta =0 and phi =0 degrees.

(d) Current Density Diagram

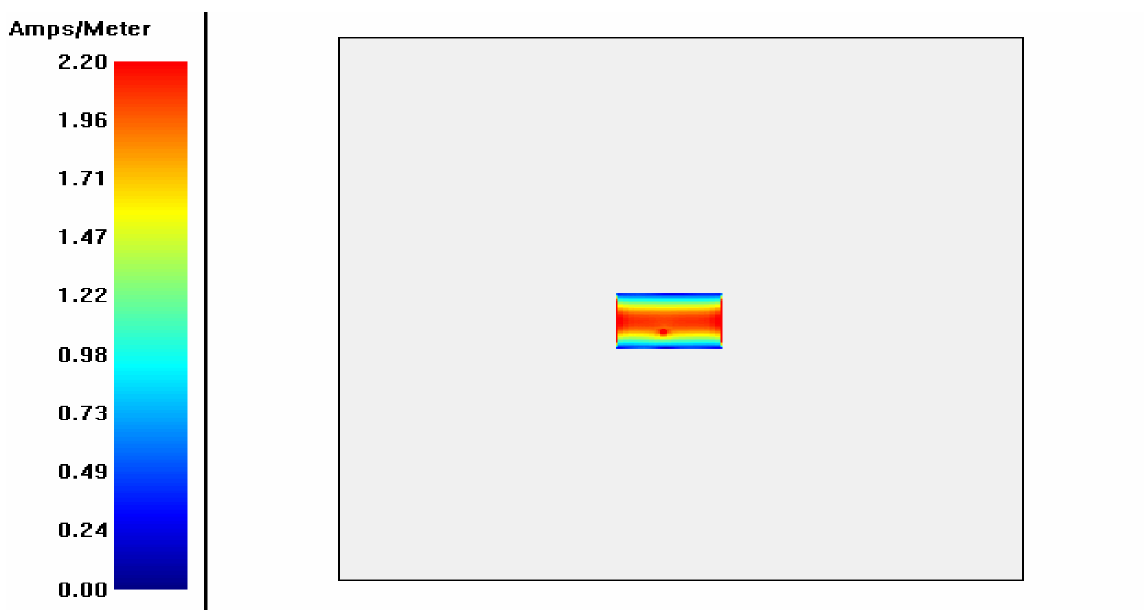


**Figure 3. 4 The current density at 3.50 GHz**

Figure 3.4 is a diagram showing the current density distribution on the patch surface. The physical meaning of current density distribution is that it is a measure how the antenna is producing a beam.

As mentioned above, the range of frequency band used in this work is 3.0-4.0GHz band. The maximum achievable bandwidth in the range 3.0-4.0GHz is 75MHz (2.29%) which agrees with the theory ‘conventional microstrip patch antennas have a bandwidth up to 3%’.

# Chapter 4

## Broadbanding Techniques of Microstrip Patch Antennas

In this chapter, eight broadbanding techniques have been explained to enhance the bandwidth of microstrip patch antennas, either by obtaining a wider bandwidth or performing a dual-band operation [3]:-

### 4.1 Parasitic Configurations

This method is chosen to investigate how the Parasitic Patch configuration [7] can improve the bandwidth of a typical microstrip antenna. In this type of antenna design, patches are placed near the edges of the original patch. These new patches may be coupled to the main patch electro-magnetically or through the direct coupling technique. Each patch can be designed in a similar manner to the original patch. The lengths of the parasitic patches will determine their resonant frequency and their width will determine the bandwidth they display at resonance.

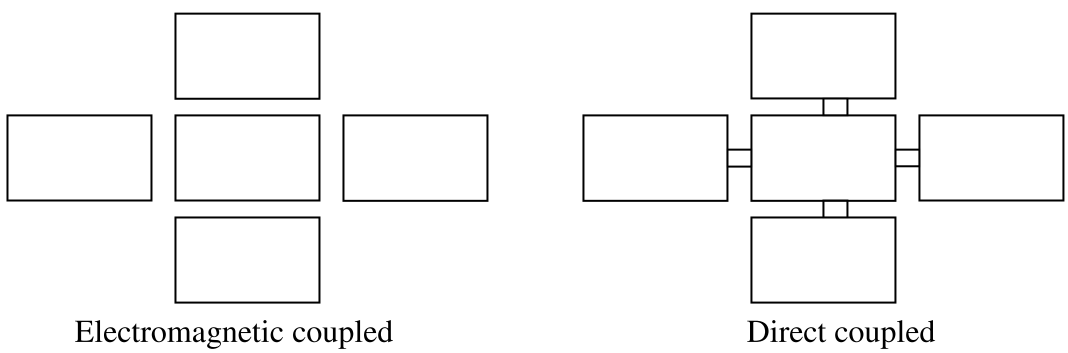


**Figure 4. 1 Basic design of microstrip patch antenna with four parasitic patches**

It should be noted that although in Figure 4.1 the patches shown are identical, each patch could have a different length and width. There was little point in changing the widths of the parasitic elements (within the scope of this project) as it only affects their individual bandwidths. And since any patches will be working together to form a broadband solution there is little need for varying their individual bandwidths. For this design of antenna each parasitic patch was considered to be of the same length. Initially a single parasitic element was used and had identical dimensions to the fed patch. The length of the elements was then altered until an acceptable result was reached. It was found during the design that it was necessary to change the feed location as it was no longer providing an optimal impedance match for the antenna with the addition of the parasitic element.

In order to get the high gain required in many applications, particularly in satellite communications, antenna arrays with large number of elements are required. This poses several problems if microstrip antenna elements are used. First if each element is connected to a feed line, the resulting feeding network will introduce unwanted radiation as well as copper losses. Second, for a phase array, each individual element will require a phase shifter in order for the beam to be steered, with the result that a great number of phase shifters are needed in large arrays. For the next generation of satellite communication antennas in which MMIC (monolithic microwave integrated circuit) devices at 20 and 30 GHz are employed in array feeds, the cost of the phase shifters is likely to be prohibitive.

The above mentioned problem may be reduced if the array is subdivided into sub-arrays. This arrangement offers the following potential advantages [7]:

- Compared to the conventional arrangement, in which every patch is fed the number of phase shifters will be reduced by a factor which is equal to the number of patches in the sub-array
- There will be much interconnecting and hence the heat loss as well as unwanted radiation will be reduced
- The parasitic elements have the effect of widening the bandwidth, with the result that the array will have a larger bandwidth than the case when each patch is fed
- These arrays are relatively simple to manufacture.

On the other hand, parasitic configurations have the following disadvantages.

- The large size, which makes them unsuitable as an array element
- The variation in the radiation pattern over the impedance BW

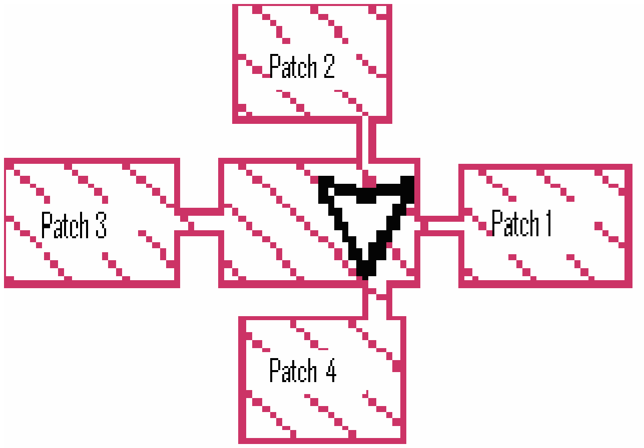


**Figure 4. 2 Geometry of a parasitic patch antenna used in the design**

## 4.2 Stacked Configurations

In the stacked configurations, two or more patches on different layers of the dielectric substrate are layered on each other. Based on coupling mechanism, these configurations are categorized as electromagnetically coupled and aperture coupled MSAs [12].

(a) **Electromagnetically Coupled MSAs**: In the electromagnetically coupled MSA, one or more patches at different dielectric layers are electromagnetically coupled to the feed line located at the bottom dielectric layer. The patch dimensions are optimized so that the resonance frequencies of the patches are close to each other to yield broad BW.

(b) **Aperture-Coupled MSAs:** In the aperture-coupled MSA [12], the field is coupled from the microstrip feed line placed on the other side of the ground plane to the radiating patch through an electrically small aperture/slot in the ground plane. The coupling to the patch from the feed line can be maximized by choosing the optimum shape of the aperture. The drawback of these structures is the increased height, which is not desirable for conformal applications and increased back radiation for aperture-coupled MSAs.

The stacked patch antenna configuration is another type that is capable of widening bandwidth as it was pointed out earlier. The general structure is shown in figure 4.3. It consists of two dielectric substrates, the feed element, a low dielectric constant foam layer (sandwiched in the middle) and the ground plane as well [3]. It is possible to increase the layers in order to get better bandwidth improvement even though the size of the antenna becomes a problem. The lower patch is fed with probe. The upper patch is electromagnetically coupled to the lower patch. The stacked structure has to be considered as two different coupled cavities. So the effect of coupling between lower and upper cavities needs to be considered in parameters that are used in the analysis. The parameters affected mainly are the dielectric constant, $\varepsilon_r$ and the dimensions of the antenna especially that of the upper patch.

The effective value of the dielectric constant, $\varepsilon_{rc}$ for a stacked structure is given by the equation [16]

$$\varepsilon_{rc} = \frac{\sum_{i=1}^{n} h_i}{\sum_{i=1}^{n} \frac{h_i}{\varepsilon_{ri}}}$$

Where, n is the number of layers in the structure. The lower and upper cavity parameters are to be analyzed separately. The analysis is done assuming that the lower cavity resembles an antenna covered by a dielectric neglecting the effects of the upper patch since the fields are concentrated in the region between the lower patch and the ground plane. When analyzing the upper patch the effects of coupling are to be taken into account. The main effect is to change the effective dimension of the patch and thus increase the resonant frequency. So the effective dimension of the upper patch is to be found by taking the expansion of the lower patch also. In resonant frequency calculation of both the patches the $\varepsilon_{reff}$ is found out using the value of $\varepsilon_{rc}$ in place of $\varepsilon_r$ i.e.

$$\varepsilon_{reff} = \frac{\varepsilon_{rc}+1}{2} + \frac{\varepsilon_{rc}-1}{2}\left[1+12\frac{h}{W}\right]^{-\frac{1}{2}}$$

Where, h is the total thickness of the substrate and W is the dimension for that patch.

| | | | |
|---|---|---|---|
| Substrate 1 | h =1.5mm | $\varepsilon_r = 2.2$ | |
| Foam | h =6.0mm | $\varepsilon_r = 1.05$ | |
| Substrate 2 | h=1.5mm | $\varepsilon_r = 2.2$ | |

Hence, the effective dielectric constant for the stacked patch configuration is

$$\varepsilon_{rc} = \frac{1.5+6.0+1.5}{\frac{1.5}{2.2}+\frac{6.0}{1.05}+\frac{1.5}{2.2}} = 1.27 \text{ and } \qquad \varepsilon_{reff} = \frac{1.27+1}{2} + \frac{1.27-1}{2}\left(1+12\frac{9}{40}\right)^{-\frac{1}{2}} = 1.205$$

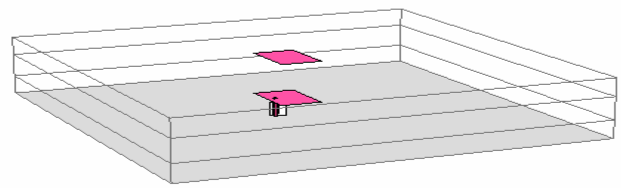

**Figure 4. 3 Geometry of stacked patch antenna**

Advantages of stacked patch antenna

- Multiple functions share common feeds
- Stagger tuning increases bandwidth
- Separately tuned radiators benefit from frequency and/or polarization isolation
- Many configurations are possible to meet a variety of needs
- Different substrates may be selected for upper and lower antenna

Disadvantages of stacked patches

- Stacked substrates must be aligned and bonded
- Increased thickness and weight of the antenna structure
- Fabrication of feed can be difficult, particularly when upper feed must attach to lower antenna

The advantages mostly relate to increases in performance, where as most of the disadvantages relate to fabrication and mechanical concerns.

## 4.3 Proximity Coupled Patch

This type is a non-contacting feeding technique that can result in wide band. As shown in Figure 4.4 two dielectric substrates are used such that the feed line is between the two substrates and the radiating patch is on top of the upper substrate. The main advantage of this feed technique [17] is that it eliminates spurious feed radiation and provides very high bandwidth (as high as due to overall increase in the thickness of the microstrip patch antenna. This scheme also provides choices between two different dielectric media, one for the patch and one for the feed line to optimize the individual performances.

Advantages

- No physical contact between feed line and radiating element.
- No drilling required.
- Less spurious radiation.
- Better for array configurations.
- Good suppression of higher order modes
- Better high frequency performance

Disadvantages

- Surface wave due to thick substrate
- Difficulty in alignment of both substrates
- Increased size of the antenna

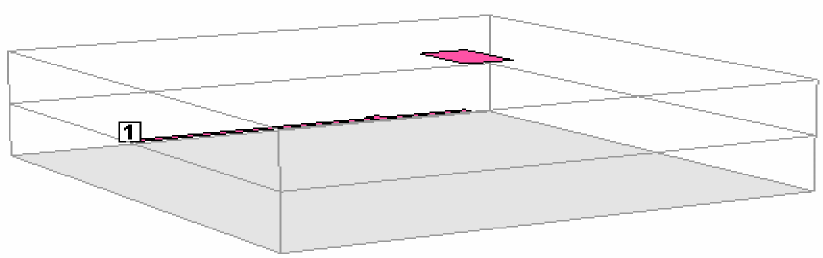


**Figure 4. 4 The schematics of proximity coupled patch antenna**

## 4.4 Specially shaped patches (E-Shaped Patch)

The regular MSA configurations, such as rectangular and circular patches can be modified to rectangular ring and circular ring, respectively to enhance the BW. The larger bandwidth is because of a reduction in the quality factor Q of the patch resonator, which is due to less energy stored beneath the patch and higher radiation.

The basic idea of such kind antenna is to modify the geometry of the typical rectangular patch antenna by inserting a pair of slits in an appropriate radiating edge to form E-Shaped patch antenna. The slits reduce the size of the original rectangular patch, because length of the current path around the slots is increased. The slots also introduces the dual frequency features, this widens the bandwidth of the proposed antenna. The higher frequency is mainly determined by central part of the proposed patch, while the lower one is controlled by the outer parts. The length, width, and position of the symmetrical slots are critical for getting wide bandwidth; otherwise only single resonant frequency will be obtained. The geometry of E-shaped antenna geometry is shown in Fig 4.5. The antenna has only one patch which is simpler than most conventional wide-band microstrip antenna which uses multiple layers. The dielectric substrate is foam material.

Advantages

- Reduced size
- High bandwidth and high gain
- Low loss (dielectric & conductor)
- Better radiation efficiency
- Surface wave excitation likely to be lowered

Disadvantages

- Large antenna volume
- Low mechanical strength

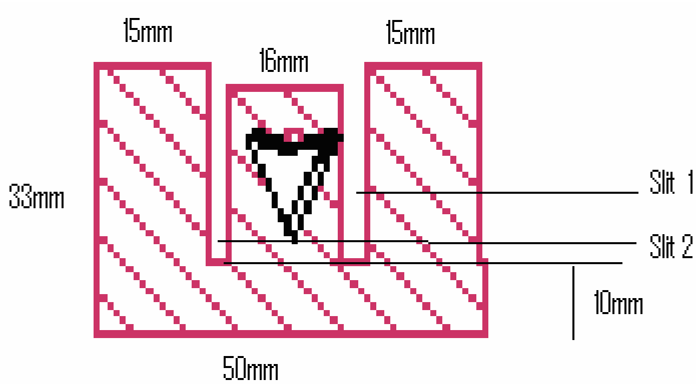


**Figure 4. 5 E-shaped patch antenna**

## 4.5 Log-Periodic MSA Configurations

The concept of log-periodic antenna [19] has been applied to MSA to obtain a multi-octave BW. In this configuration, the patch dimensions are increased logarithmically and the subsequent patches are fed at 180 deg out of phase with respect to the pervious patch. In this structure, the low and high frequency limits of the bandwidth are set by the largest and smallest dimensions of the structure, respectively. The quasi-log-periodic antenna was achieved by arraying different narrow bandwidth radiators, each having its own frequency band of operation. The main advantages are the absence of an array effect in the E-plane and the fact that the antenna can be designed for a specified degree of matching by the proper choice of spacing between the resonant frequencies, namely, the log-periodic expansion factor. But a considerable part of the input power reaches the end of the feed line, which was not terminated in an attempt to maintain the high efficiency. Application of the log-periodic principles to an array involves several inherent problems, with the constant substrate thickness as the most apparent difficulty. In this case, the substrate thickness was kept constant, but the traveling-wave effect was not considered in the network analysis. If more than a few elements are used, the feed end will become too long for some elements and the performance will deteriorate. Yet, the increase in size may not justify what this antenna can offer, and the radiation patterns also vary strongly with frequency.

## 4.6 Use of diodes

The use of Varactor diodes to perform dual-frequency operation is another wideband technique. Two diodes are positioned symmetrically in the patch to minimize the cross-polarization effects, and the relationship between the power and the bias voltage level of the Varactor diodes represents a way of tuning the structure. The flaws of this technique are the dependence of the resonant frequencies on the position of the diodes and, hence, the lack of versatility, along with difficulties in the manufacturing process and nonlinearity problems in high power applications. Similarly, the effects of an optically controlled PIN diode were incorporated into a model. The complexity of this technique, although compatible with MMIC structures, is apparent.

## 4.7 Stacked-Parasitic MSAs

The stacked-parasitic [3] techniques are combined further to increase the bandwidth and gain. A probe-fed single rectangular or circular patch located on the bottom layer has been used to excite multiple rectangular or circular patches on the top layer, respectively. These provide an increase in gain, besides increasing the BW.

## 4.8 Impedance Matching Networks for Broadband MSAs

The impedance-matching networks are used to increase BW of the MSA [3] and [20]. Some examples that provide about 10% BW are the rectangular MSA with a coplanar microstrip impedance matching network and an electromagnetically coupled MSA with single-stub matching.

In the next section, broad banding techniques such as stacked patch antenna, parasitic patches, proximity coupled patch and an E-shaped antennas are examined and the results obtained are illustrated graphically in the subsequent chapter.

# Chapter 5

# Simulation Results and Discussions

## 5.1 About Application of *SONNET* to *Free Space* Radiation Problems

The SONNET algorithm is designed to treat planar circuits that operate inside a rectangular conducting box. Therefore, the extension to free space radiation problems is not obvious. However, the SONNET User's Manual [18] lists five conditions under which a free space approximation is valid. The conditions are easily violated, and unless the analysis is carefully prepared, the algorithm is likely to yield incorrect results. However, when all five guidelines are satisfied, useful, but approximate, results for input impedance and far-field radiation pattern are obtained.

***First Condition:*** *Both of the lateral substrate dimensions must be greater than one or two wavelengths* [18].

If the walls that make up the waveguides are too close together, the number of non-vanishing homogenous modes in the summation is limited. This is not the free space condition and impedance and pattern calculations are corrupted.

***Second Condition:*** *The sidewalls of the conducting box must be far enough from the radiating structure so that that they have no effect* [18].

If the walls of the waveguide are close to the radiating structure, surface currents are coupled to them. The result is an imaging effect that creates the equivalent of another radiating structure behind the sidewall. Therefore, the sidewall spacing, which is equivalent to the substrate dimensions, must be as large as possible.

***Third Condition:*** *Place the top cover outside the near field of the radiating structure.*

This condition prevents the resistive top cover of the waveguide from interfering with the reactive near fields of the radiating structure. If the condition is violated, the input reactance is invalid. The top cover spacing must be at least a half-wavelength to satisfy this condition.

***Fourth Condition:*** *Set the top cover resistivity to 377 Ohms/square* [18].

This matches the resistance of the top cover, $Z_{tc}$ to that of free space ($\eta = 377\Omega$). Thus, the top cover is effectively removed and resonances due to the closed box are avoided.

However, $Z_{tc} = 377\Omega$ is a compromise because TE modes have modal impedances higher than 377 Ω, and TM modes have modal impedances lower than 377 Ω. If the waveguide is large in both lateral dimensions (condition 1), all of the modal impedances approach $377\Omega$, and reflection from the top cover is minimized. The effect is further limited if the top cover is located far away from the radiating structure i.e. the top cover is much greater than the operating wave length.

***Fifth Condition:*** *The surface can not generate a significant surface wave* [18].

This is true because surface waves will be reflected by the conducting sidewalls and will cause inaccurate results. Surface waves are generated within thick substrates. Therefore, when thick dielectric substrates are used special attention is required to verify the absence of surface wave effects in the results.

## 5.2 Simulation Results and Discussions

Four of the broadbanding techniques that have been explained in chapter 4 are selected and analyzed thoroughly. These are the parasitic patches, the stacked patches, the proximity coupled patch and the E-shaped type patch. The simulation results of each of the antennas are presented below in the subsequent sections. Finally, the results are summarized and discussed.

### 5.2.1 Parasitic patch antennas

The following results are obtained for the parasitic patch type antenna. The results are explained in terms of the return loss, input impedance and radiation pattern. The current density on the antenna is also displayed.

(a) Return Loss Curve

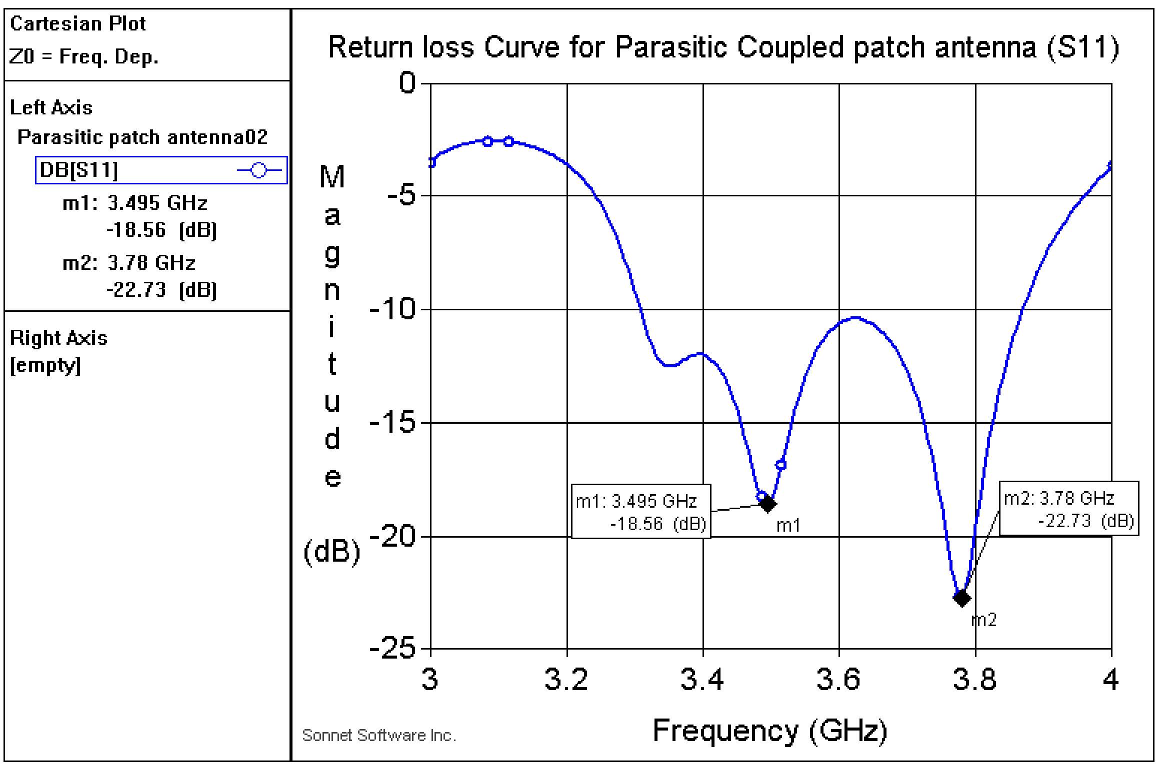


**Figure 5. 1 Simulated RL of parasitic coupled patch**

As we see from the graph the bandwidth obtained using parasitic microstrip patch antenna is about 560MHz which is nearly 15.6% of the center frequency of the driven patch.

(b) Input Impedance Curve

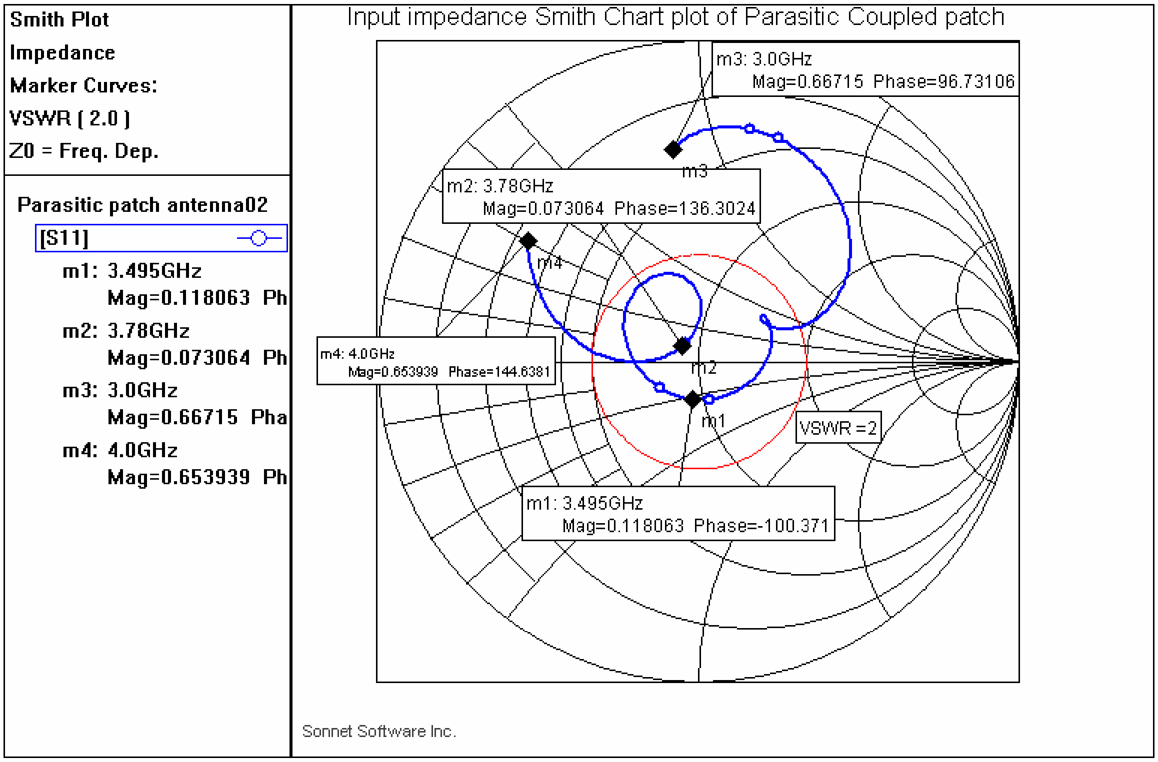


**Figure 5. 2 Input impedance curve of parasitic coupled patch antenna**

The input impedance curve tells us the magnitude and phase angle of the input impedance of the antenna at the respective frequencies. It is also possible to estimate the bandwidth of the antenna from this graph by reading the frequencies at the points where the VSWR=2 circle and the input impedance curve intersect.

(c) Radiation Pattern Plot

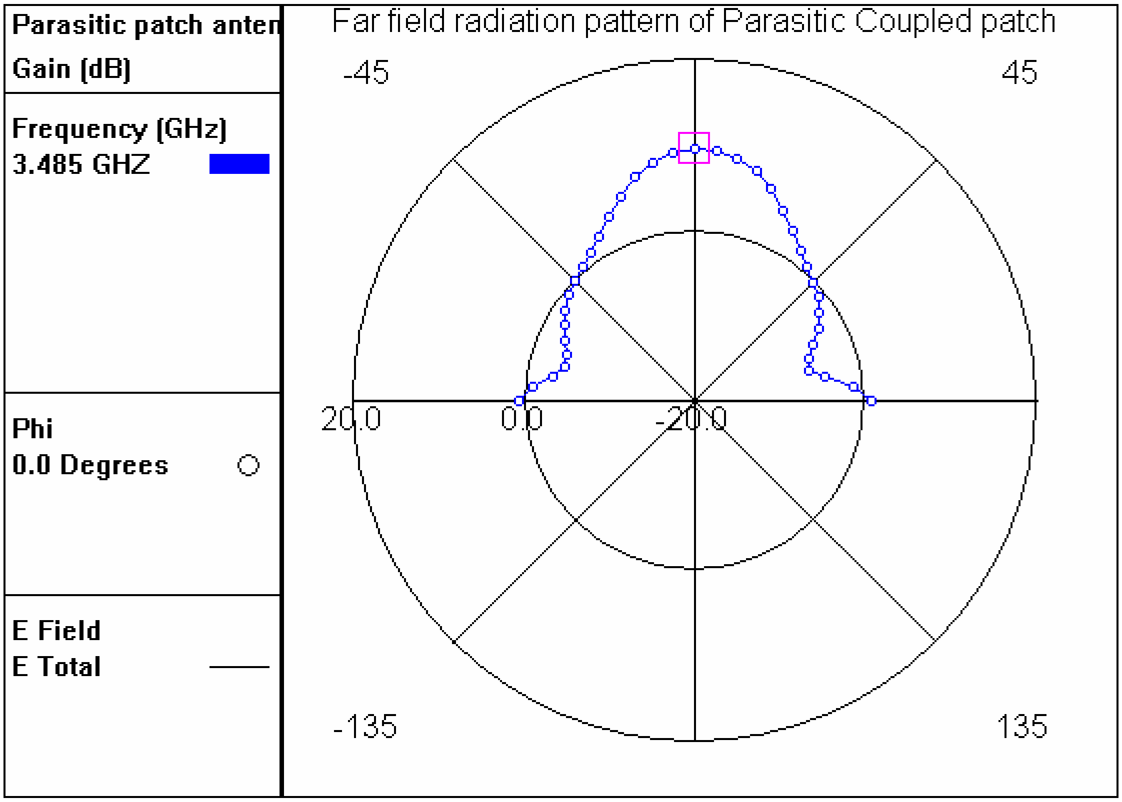


**Figure 5. 3 Radiation pattern of the parasitic coupled patch**

The radiation pattern plot of an antenna tells us the gain obtained at the respective operating frequency. It is a plot of the antenna gain versus the elevation angle. The antenna has a gain of 9.62dBi at 3.485GHz $\theta = 0^0$ *and* $\phi = 0^0$.

(d) Current density Diagram

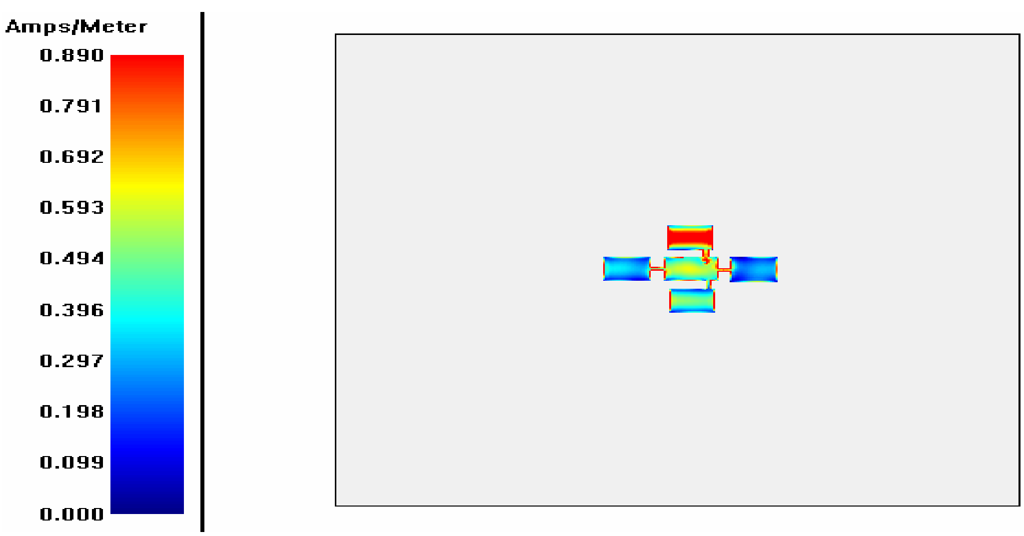


**Figure 5. 4 Current density diagram of the parasitic coupled patch at 3.845GHz**

### 5.2.2 Stacked patch antenna

(a) Return Loss Curve

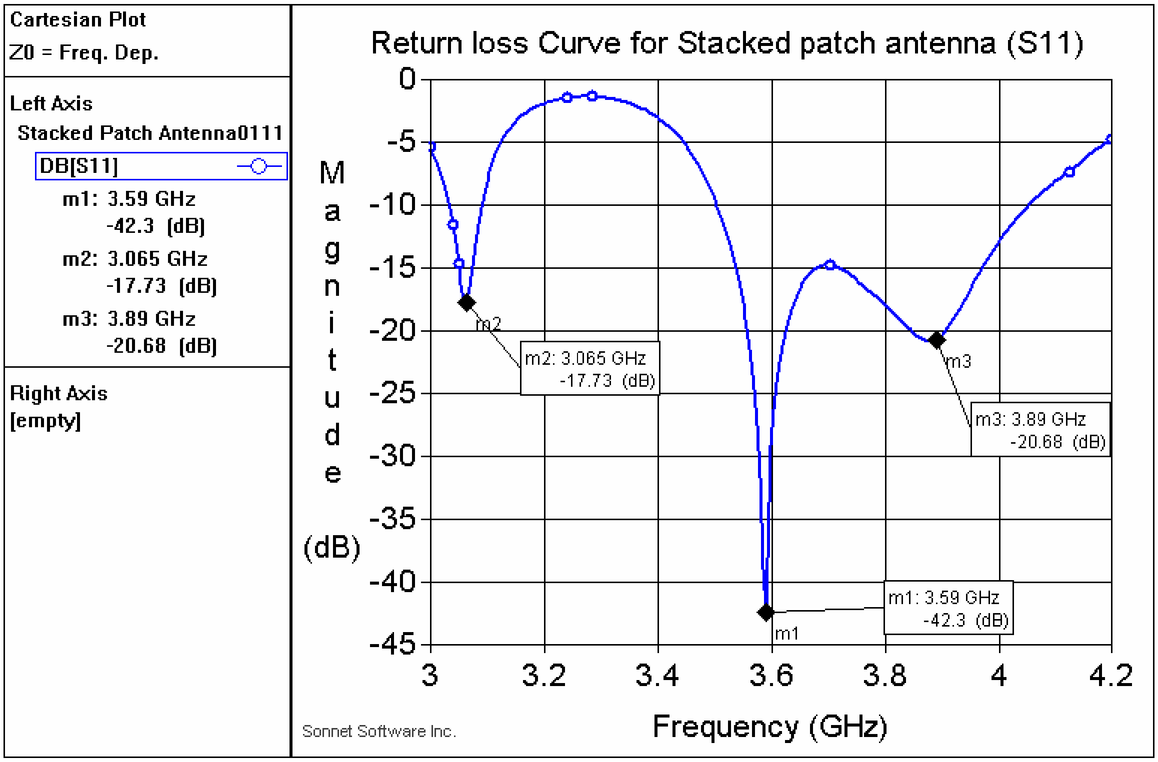


**Figure 5. 5 Simulated RL of the stacked patch antenna**

It is observed from the graph that this antenna improved the bandwidth of the original patch to 550MHz. It resulted in 11.5% of the center frequency.

(b) Input Impedance plot

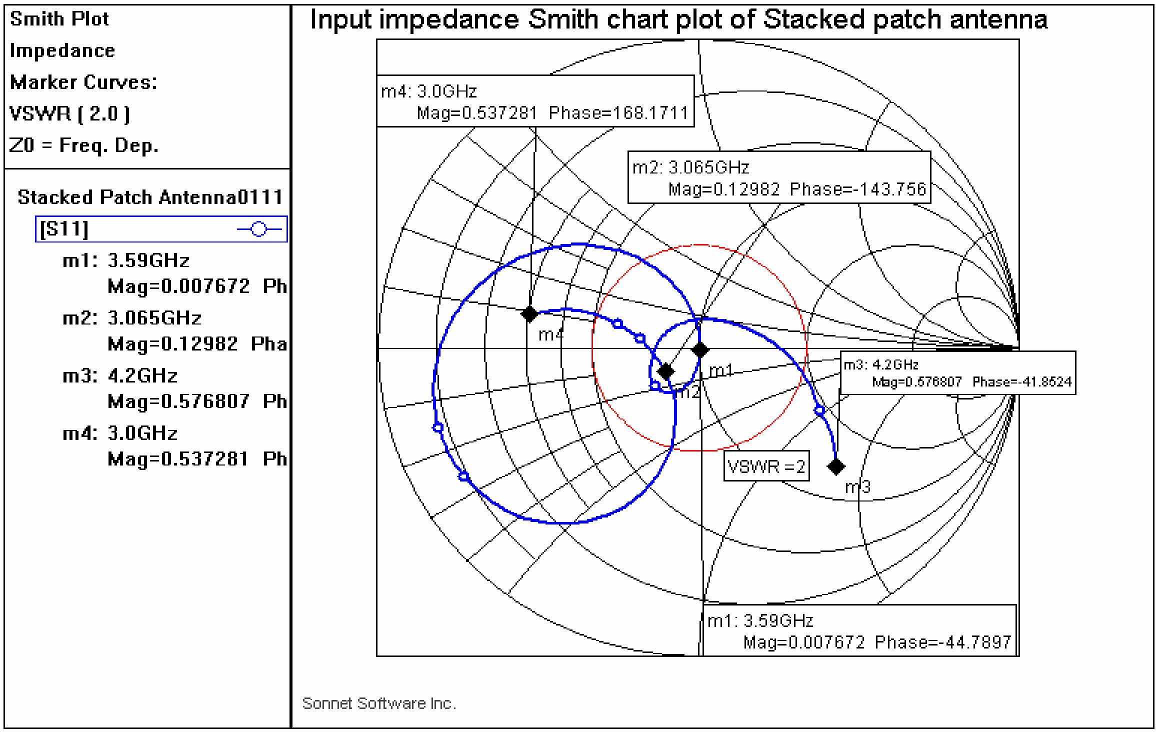


**Figure 5. 6 Input impedance curve of stacked patch antenna**

(c) Radiation Pattern plot

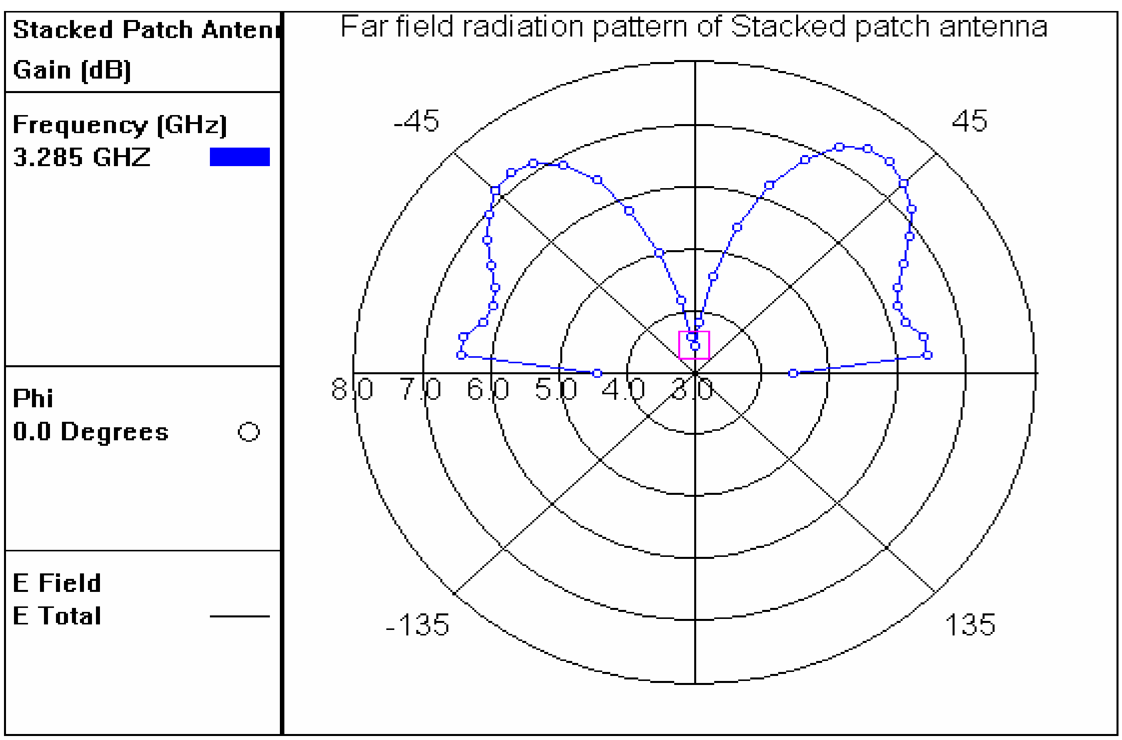


**Figure 5. 7 Far field radiation pattern of stacked patch antenna**

The gain for the stacked patch antenna is about 3.425dBi as it is evident from the graph at $\theta = 0^0$ *and* $\phi = 0^0$.

(d) Current Density Diagram

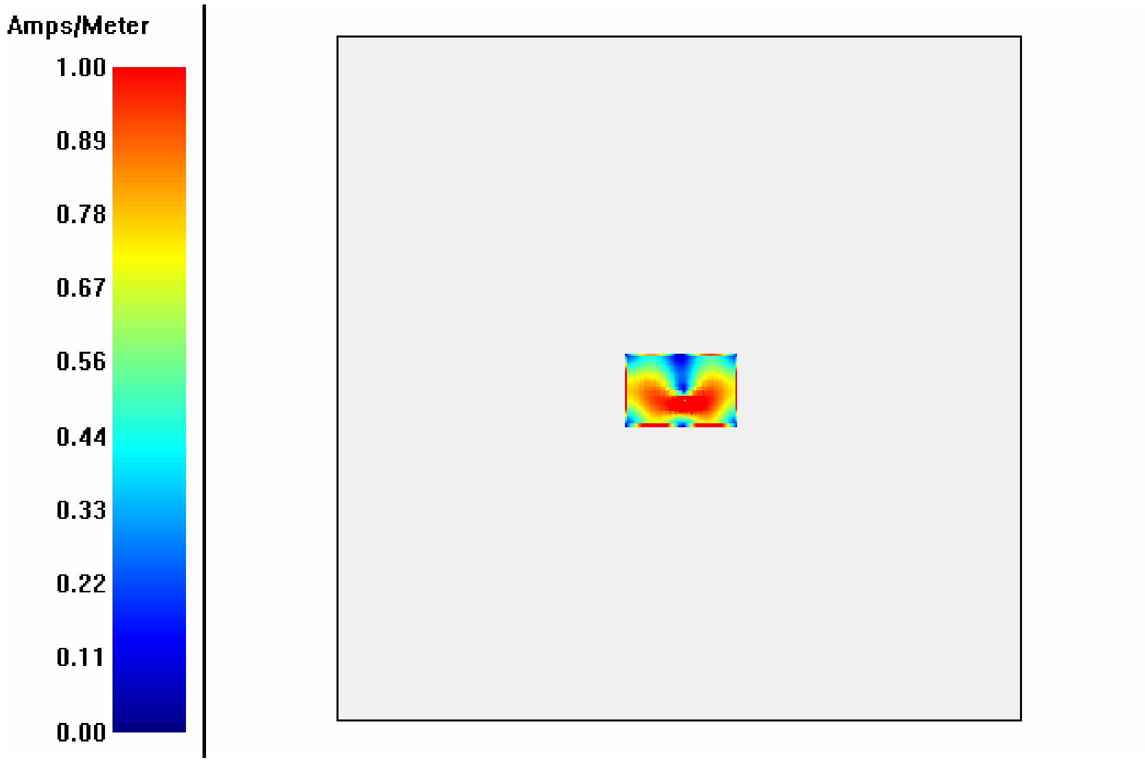


**Figure 5. 8 Current density diagram of stacked patch antenna at 3.285GHz**

### 5.2.3 Proximity coupled patch

(a) Return Loss Curve

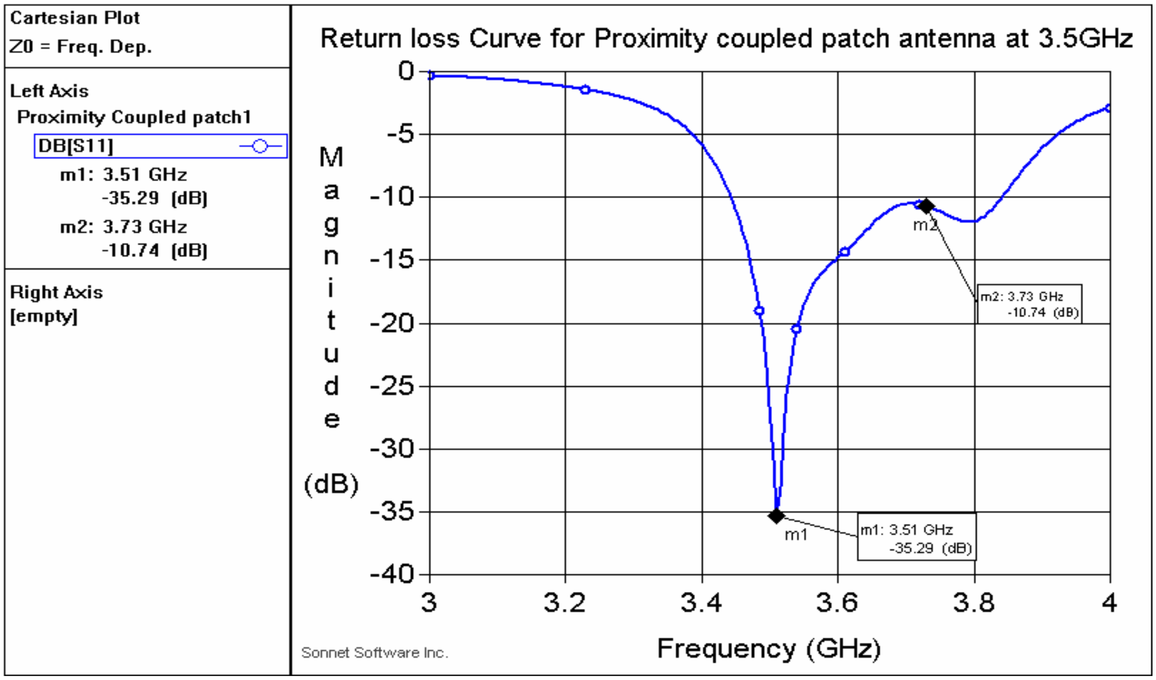


**Figure 5. 9 Simulated RL of the proximity coupled patch**

This antenna has increased the bandwidth to 400MHz i.e. 10.8% of the center frequency.

(b) Input Impedance Curve

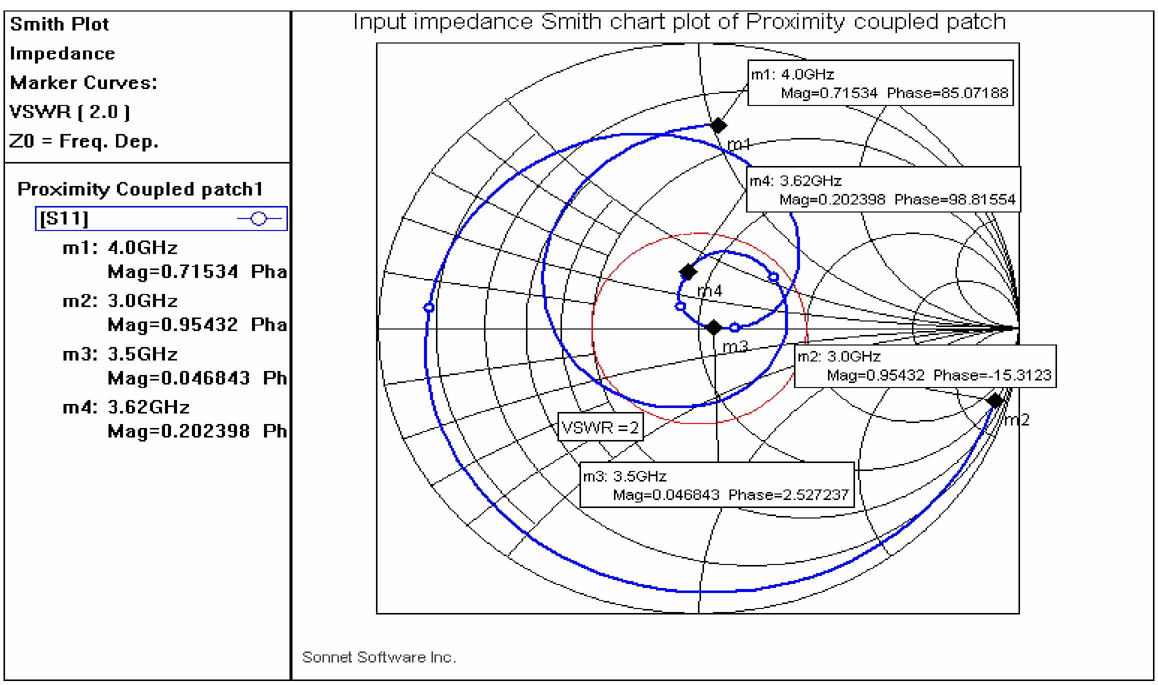


**Figure 5. 10 Input Impedance curve for proximity coupled patch**

(c) Radiation Pattern plot

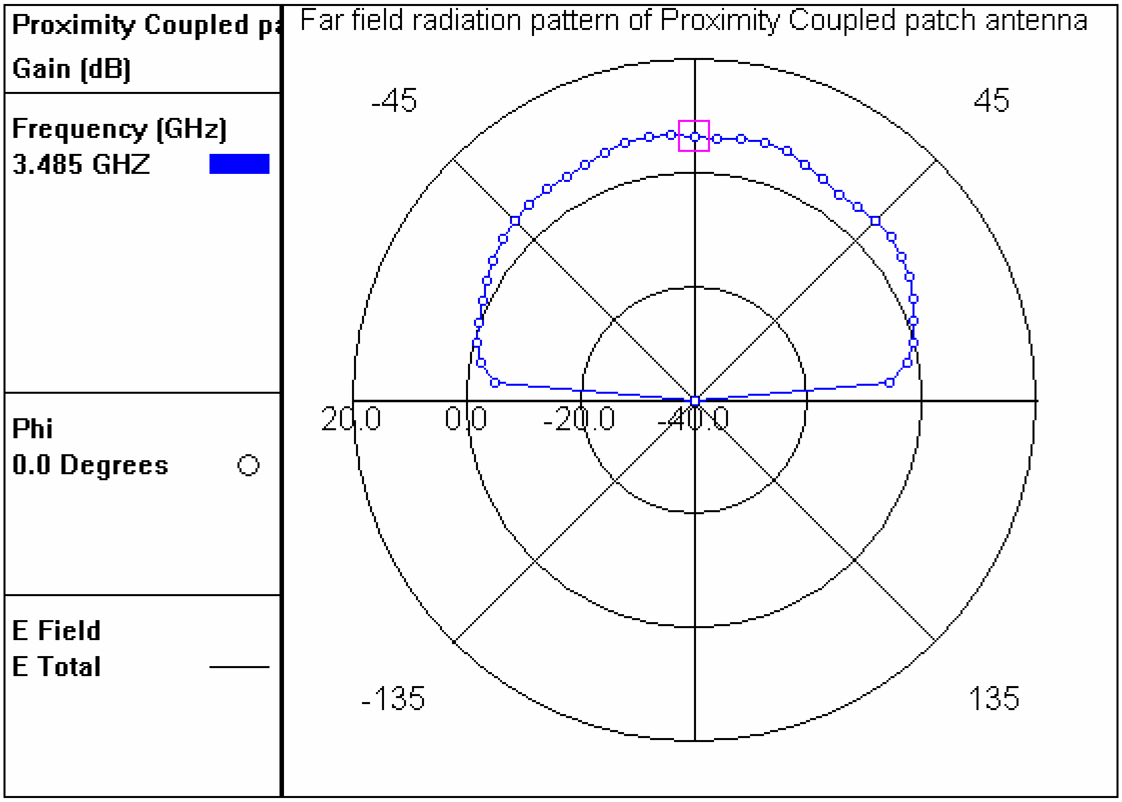


**Figure 5. 11 The radiation pattern of the proximity coupled antenna**

The proximity coupled patch antenna has a gain of 6.29 dBi at 3.485GHz with $\theta = 0^0$ *and* $\phi = 0^0$.

(d) Current Density Diagram

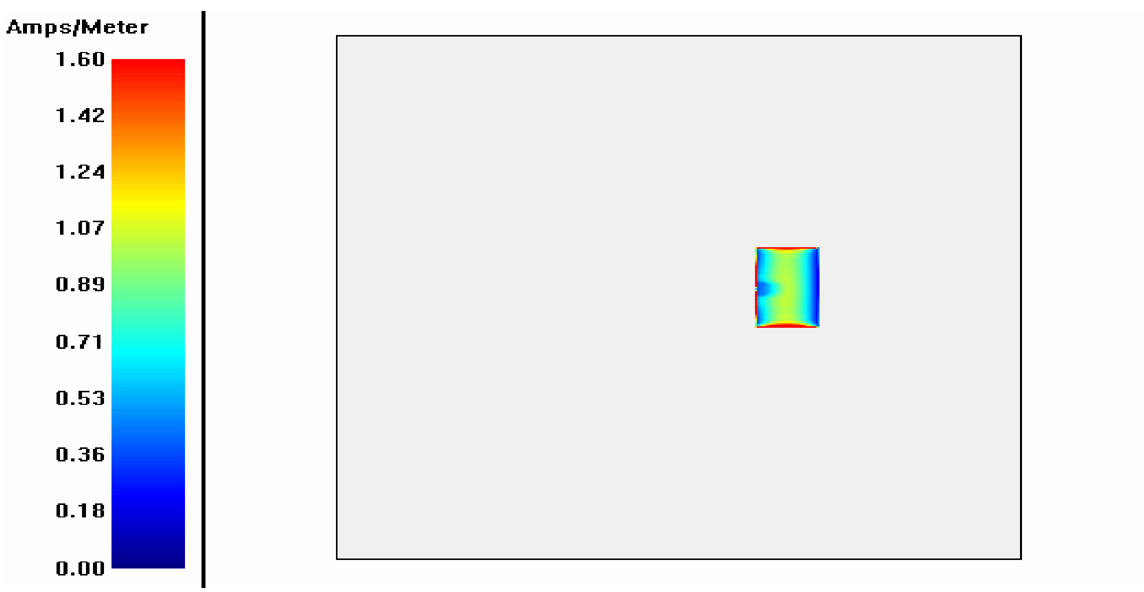


**Figure 5. 12 The current density diagram of proximity coupled at 3.485GHz**

### 5.2.4 E-shaped patch antenna

(a) Return Loss Curve

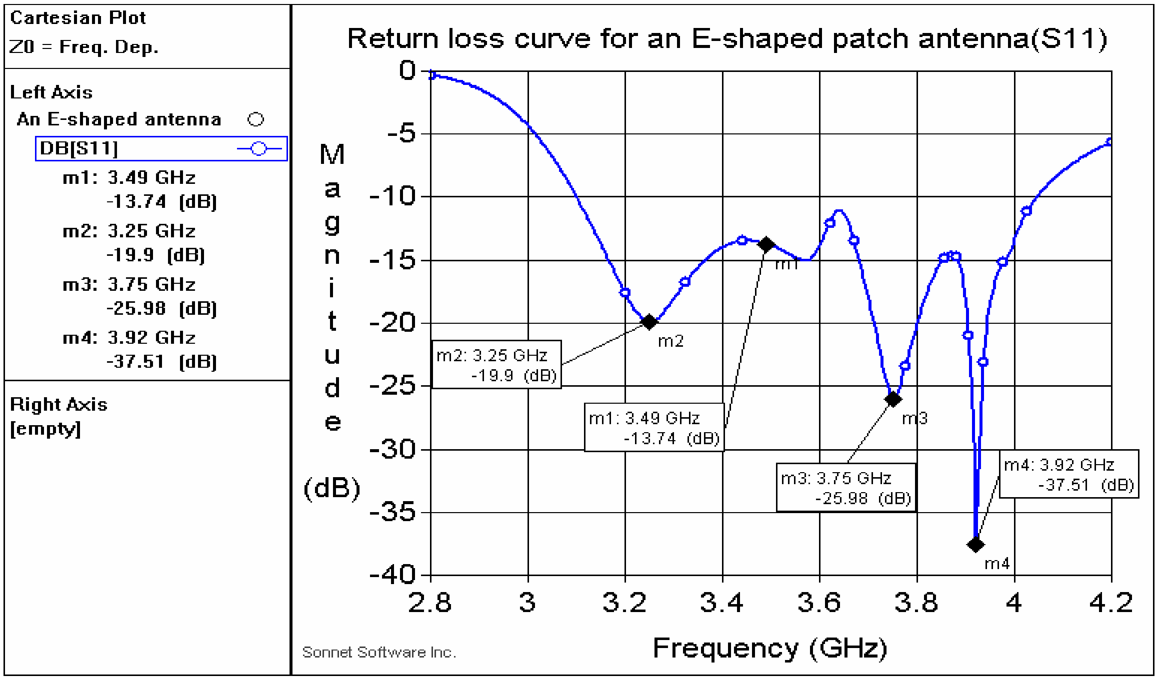


**Figure 5. 13 Simulated Return losses of E-shaped patch antenna**

As it seen from the return loss curve bandwidth obtained in this case is about 950MHz more than 25.6% of the center frequency.

(b) Input Impedance Curve

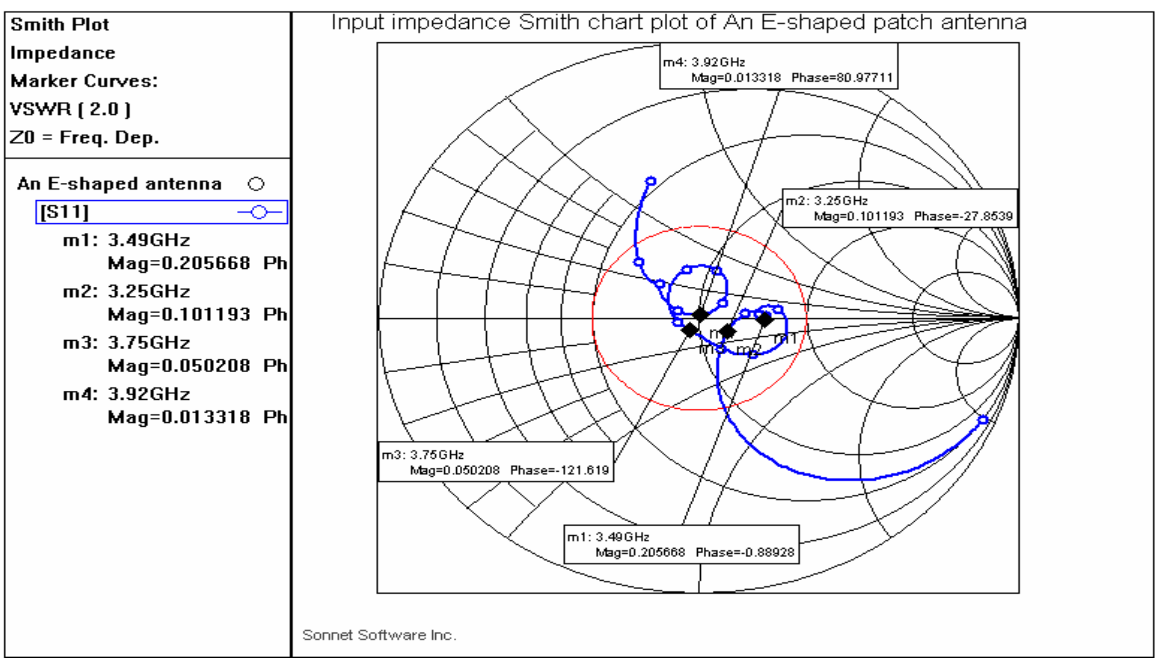


**Figure 5. 14 The impedance curve of E-shaped patch antenna**

(c) Radiation Pattern Plot

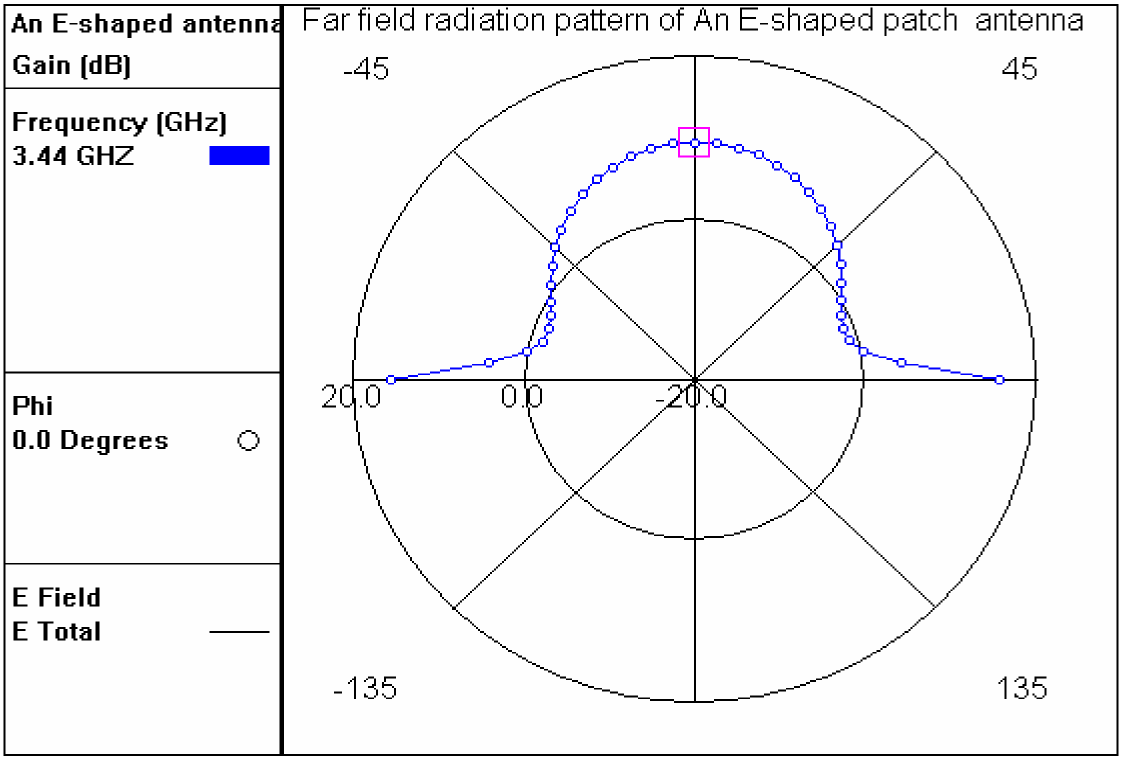


**Figure 5. 15 Radiation pattern for the E-shaped patch antenna**

The gain of this E-shaped patch is 9.42dBi at 3.44GHz $\theta = 0^0$ *and* $\phi = 0^0$.

(d) Current Density

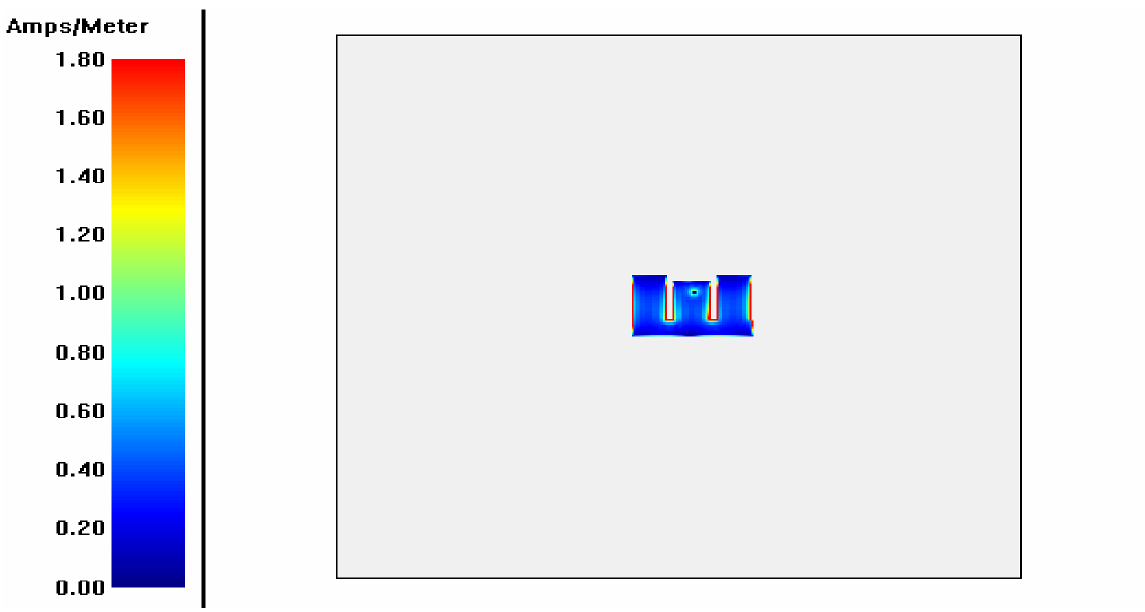


**Figure 5. 16 Current density diagram for the E-shaped antenna at 3.44GHz**

### 5.2.5 Discussion of Results

The following table summarizes the values of parameters used in the analysis and the simulation output results obtained in the previous section.

**Table 1**

| Antenna Type | Proximity Coupled | Stacked Patches | Parasitic Coupled | E-shaped Patch |
|---|---|---|---|---|
| Dielectric Material | RT 5800 | RT 5880 | RT 5800 | Foam |
| Dielectric Constant | 2.2 | 2.2,1.05, 2.2 | 2.2 | 1.05 |
| Substrate thickness (mm) | 3.2 | 9.0 | 4.0 | 8.0 |
| Loss tangent | 0.0009 | 0.0009 | 0.0009 | 0.0001 |
| Resonant frequency(GHz) | 3.5 | 3.59 | 3.5 | 3.5 |
| Bandwidth (MHz) | 400 | 550 | 560 | 950 |
| Gain (dBi) | 6.29 | 3.425 | 9.625 | 9.51 |

*1. Parasitic Patch antenna*

The parasitic patch antenna in this thesis is made of a single dielectric layer. On the dielectric substrate five patches are laid. The central patch is the driven patch and it is directly fed with a via port (i.e. a coaxial port). The parasitic patches are directly coupled to the central patch for the criticality of coupling. The parasitic patch arrangement is depicted in Figure 4.2. The central patch is 27mm by 40mm. To get wide band property the width of the parasitic patches are made different from on another but the length is kept constant.

The connecting metallic strips also have some effects on the performance of the antenna. Because the strip lines are a source of unwanted radiation and conductor loss if their dimensions is not appropriately selected. Hence the current dimensions of these strips lines used in the design of this antenna are obtained after several iterations. The dimensions of the strip lines are chosen in such away that to minimize the matching problem and to get acceptable performance.

Another factor that influences the bandwidth is the substrate thickness h. This is adjusted to 4mm which is unlikely to produce surface wave.

The dielectric constant of the substrate material also is taken in to consideration for higher bandwidth. Increasing the dielectric constant of the substrate decreases the bandwidth of the antenna with the advantage of compact antenna. On the other hand, decreasing the dielectric constant produces wide band with larger antenna dimensions.

The dimensions $(in\,mm)$ of the patches in the parasitic configuration are listed in the table below:

| Driven patch | Patch 1 | Patch 2 | Patch 3 | Patch 4 |
|---|---|---|---|---|
| 27 x 40 | 27 x 33 | 27 x 31 | 27 x 34 | 27 x 31 |

The bandwidth and gain obtained in the simulation are 560MHz and 9.625dBi respectively.

### *2. Stacked Patch antenna*

The stacked patch antenna depicted in Figure 4.3 consists of two dielectric substrates and two radiating elements. The lower patch is fed by a coax. The upper one is coupled to the lower electromagnetically. In the middle of the two dielectric substrates a foam layer of low dielectric substrate constant is placed to reduce the surface wave excitation. As it is observed in section 4.2 the effective dielectric constant reduces to 1.205. The decrease in the effective dielectric substrate is an indication for larger bandwidth. The metallic patches are designed on this basis. After the analysis completes the Smith chart revealed there are unmatched conditions. That is, the input impedance curve is getting inductive and far away from the center or the Smith Chart.

This is overcome by the addition of a passive component (in this case capacitor is used 0.99pF) and better performance has been obtained. The resulting bandwidth and antenna gain are 550MHz and 3.425dBi respectively. The gain is lowered due to the overall thickness of the substrate.

### *3. Proximity Coupled Patch antenna*

The proximity coupled patch has a simplest geometry depicted in Figure 4.4 contains two dielectric substrates, a feed element (Microstrip line feed) and the patch. Each substrate is 1.6mm thick. The dielectric substrate constant is 2.2 for both substrates. The patch is designed for 3.5GHz and the dimension of the patch is 27 by 40 mm. The bandwidth determining factors as already mentioned are the patch dimensions (the length and the width), the dielectric substrate thickness and the dielectric constant. Only the width of the antenna is selected for wide band *i.e.* $W = 1.5L$ . The rest parameters are being held constant. The width (6mm) of the feed line is selected appropriately to reduce the conductor loss and for optimum band width.

After the completion of the analysis the input impedance on the Smith chart showed the necessity of matching since the impedance locus is more capacitive. An inductance of 0.5nH is used for compensation that results in upward shift of the impedance locus. As a result wider bandwidth of 400MHz with 6.25dBi gain is achieved.

### 4. *E-shaped Patch antenna*

The fourth type of antenna is an E-shaped patch type depicted in Figure 4.5. The original type of antenna is modified to result that shape. The important dimensions are already shown on the Figure. As the simulation results indicate the antenna has wide band with different frequency points on which the antenna attain good performance. This is due to the introduction of different resonating parts on the patch.

This antenna seems to be a combination of four patches:

- (i) a patch of dimensions 10mm by 50mm
- (ii) patches of two 15mm by 23mm
- (iii) a patch of 16mm by 19mm

Therefore, the four patches operate on different frequencies, which is able to result in wide band. This antenna confirms the combination of multi-resonant elements yield better bandwidth.

The dielectric constant of the dielectric material used in the E-shaped patch is very low *i.e.* $\varepsilon_r = 1.05$ which contributes positively for the study. Since the dielectric constant is significantly low there is low probability of surface wave excitation. The patch dimensions shown on the diagram of the E-shaped antenna were also selected for optimum performance.

The substrate thickness is 8mm. An inductance of 0.5nH is used to balance the feed elements capacitive effect and to bring the impedance locus near the center of the Smith chart for better performance. The gain and the bandwidth of this antenna are respectively, 9.51dBi and 950 MHz.

The parameters of interest in an antenna are the bandwidth and the gain. As we can see from the table the in terms bandwidth

$$\Pr oximity\, Coupled\ Patch < Stacked\ Patch < Parasitic\, Coupled\ Patch < E - shaped\ Patch$$

The E-shaped patch antenna thus gives us the desirable features that a good antenna can have. Some of the features are light weight, low loss, high gain and wide band etc.

# Chapter 6

## 6.1 Conclusions

In Chapter 2 basic ideas about microstrip patch antenna, its working principle and important parameters have been discussed. The third chapter explained the analysis and designs a typical patch antenna that helps describing its narrow bandwidth problem as well. Chapter 4 reviews the different types of broadbanding techniques by providing the relative merits and demerits respectively. Simulation results are discussed in chapter 5.

The thesis work aimed at improving the bandwidth of microstrip patch antennas. Out of the different types of broad-banding techniques that help alleviate the narrowband limitation of such antenna, four techniques were selected and analyzed. The results obtained clearly indicate the main factors that affect the bandwidth of a particular microstrip antenna are thickness of the dielectric substrate, the size of the metallic patch, the dielectric constant of the dielectric substrate, the feed type to be used (as seen in the non-contacting feed techniques) and the coupling level to some extent.

As it was observed in Chapter 5 of this thesis the bandwidth is significantly improved after the application of the techniques described in Chapter 4. To name those techniques parasitic coupled patches, stacked patches, proximity coupled patches and an E-shaped patch antenna.

One of the challenging situations encountered in the design of each of patch antennas is to obtain the exact location of the feed element (port) and to get better coupling in the case of multi-layer configuration. The feed point is located at the point where better antenna performance is obtained, since there is no closed mathematical formulas that help determine the correct feed point location.

Another difficulty in designing patch antenna is also maintaining all the antenna parameters at the desired level. This, of course, is very difficult. For example while I search for larger bandwidth the antenna gain may go down. If we need a compact and size reduced antenna we should sacrifice the bandwidth. Therefore, it is unquestionable to set some tradeoffs among size, geometry and the antenna parameters in all aspects. So in the design I tried to balance the trade offs the have been discussed in Chapter 3.

The third challenge was to get approximately the operating frequency of the original antenna after the application of each of the broadbanding techniques. To overcome this problem each of the antennas has been tuned using passive circuit elements wherever it was necessary.

The data listed in Table 1 is used in the antennas design and the expected simulation results confirmed the required result is acceptable. The return loss curve is used as a measurement criterion for the performance of each of the antenna. Hence, for better performance (*physical S-parameter*) the return loss is measured at $-9.5\,dB\,(VSWR < 2)$ and the corresponding frequency band is read by drawing horizontal line through the $-9.5dB$ point. The results obtained (*bandwidths for each antenna*) are listed in Table 1.

In general, from the simulation results obtained, the antenna having a thicker dielectric substrate and lower dielectric constant result in wider bandwidth. When the dielectric substrate is replaced by low dielectric constant foam material both bandwidth improvement and surface wave reduction seen as it is observed in the E-type antenna. Wide bandwidth in this antenna is also the effect of removing some metallic part from the patch which creates larger current path. The E-type antenna is recommended as being better in all aspects.

The antenna designed through out this thesis can be applied in a *WLAN*.

## 6.2 Recommendations for Future Works

Further studies can be carried out on the following issues:

1. The gain and efficiency of the antenna analyzed are relatively small. Hence it needs some improvement.
2. Surface wave reduction
3. Optimization of the antenna by varying the feed elements
4. To reduce the antenna size by using dielectric substrates having higher dielectric constants and using a method of shorting posts

## Appendix A

### Documentation

| Antenna | Parasitic | Stacked | Proximity | E-shaped |
|---|---|---|---|---|
| Box size | 520 by 520 mm (54 mm high) | 290 by 290 mm (59 mm high) | 264 by 264 mm (53.2 mm high) | 300 by 300 mm (80 mm high) |
| Cell size (# cells) | 1 by 1 mm | 1 by 1 mm | 0.2 by 0.2 mm | 0.2 by 0.2 mm |
| Top of Box | Free Space | Free Space | Free Space | Free Space |
| No of Dielectrics | 2 (1 metallization level) | 4 (3 metallization levels) | 3 (2 metallization levels) | 2 (1 metallization levels) |
| Metals used | Lossless | Lossless | Lossless | Lossless |
| No of polygons | 2 (all staircase) | 3 (all staircase) | 2 (all staircase) | 2 (all staircase) |
| Dielectric material | RT 5880 | RT 5880 and foam | RT 5880 | Foam |
| Substrate thickness | 4 mm | 9mm | 3.2mm | 8mm |
| Dielectric constant | 2.2 | 2.21.05,2.2 | 2.2 | 1.05 |
| Dielectric loss tangent | 0.0009 | 0.0009 | 0.0009 | 0.0000 |
| Sweep | 3.0 to 4.0 GHz ABS | 3 to 4.2 GHz ABS | 3.0 to 4.0 GHz ABS | 2.8 to 4.2 GHz ABS |
| Number of ports | 1 | 1 | 1 | 1 |
| De-embed | Yes | Yes | Yes | Yes |

| | | | | |
|---|---|---|---|---|
| Speed/Memory Vs Accuracy | slowest analysis/more memory maximum accuracy | slowest analysis/more memory maximum accuracy | slowest analysis/more memory maximum accuracy | slowest analysis/more memory maximum accuracy |
| Maximum Subsection size | 20 Subs/Lambda | 20 Subs/Lambda | 20 Subs/Lambda | 20 Subs/Lambda |
| Sub-sectioning Frequency | Present Analysis Only | Present Analysis Only | Present Analysis Only | Present Analysis Only |
| Frequency Band | 3 - 4 GHz | 3 – 4.2 GHz | 3 - 4 GHz | 3.2 - 4.2 GHz |
| Estimated Memory | 114 MB | 43 MB | 116 MB | 84 MB |
| Subsections | 3612 | 2144 | 3076 | 2163 |
| Analysis Time | 13 minutes 13 seconds (1 minute 53 seconds per analysis) | 3 minutes 47 seconds (28 seconds per analysis) | 17 minutes 54 seconds (2 minutes 33 seconds per analysis) | 26 minutes 55 seconds (2 minutes 4 seconds per analysis) |

# Appendix B

## Antenna Fundamentals

In this chapter, the basic concept of an antenna is provided and its working principle is explained. Next, some critical performance parameters of antennas are discussed.

### B.1 What is an antenna?

An antenna is a "transducer" between the electromagnetic waves in space and the voltages or currents in a transmission line. When transmitting, the antenna converts the electric signals into radio waves; a receiving antenna reverses the process and transforms the radio waves back into electric signals. Most antennas are passive and are simple metal structures that launch or collect the radio waves. According to the "reciprocity" principle from which the receiving properties of a passive antenna can be derived from its transmitting properties and conversely, all passive antennas can transmit and receive indifferently the electromagnetic waves.

### B.2 How an Antenna radiates

In order to know how an antenna radiates, let us first consider how radiation occurs. A conducting wire radiates mainly because of time-varying current or an acceleration (or deceleration) of charge. If there is no motion of charges in a wire, no radiation takes place, since no flow of current occurs. Radiation will not occur even if charges are moving with uniform velocity along a straight wire. However, charges moving with uniform velocity along a curved or bent wire will produce radiation. If the charge is oscillating with time, then radiation occurs even along a straight wire as explained by Balanis [1].

The radiation from an antenna can be explained with the help of Figure B.1 which shows a voltage source connected to a two conductor transmission line. When a sinusoidal voltage is applied across the transmission line, an electric field is created which is sinusoidal in nature and this results in the creation of electric lines of force which are tangential to the electric field. The magnitude of the electric field is indicated by the bunching of the electric lines of force. The free electrons on the conductors are forcibly displaced by the electric lines of force and the movement of these charges causes the flow of current which in turn leads to the creation of a magnetic field.

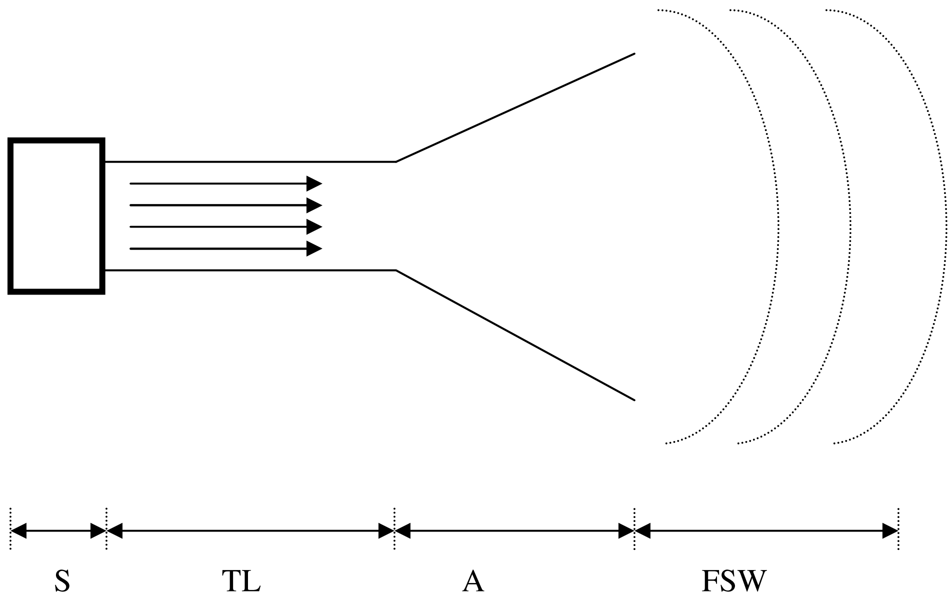


**Figure B. 1 Radiation from an antenna (S=source, TL= transmission line, A= antenna and FSW= free space wave).**

Due to the time varying electric and magnetic fields, electromagnetic waves are created and these travel between the conductors. As these waves approach open space, free space waves are formed by connecting the open ends of the electric lines. Since the sinusoidal source continuously creates the electric disturbance, electromagnetic waves are created continuously and these travel through the transmission line, through the antenna and are radiated into the free space. Inside the transmission line and the antenna, the electromagnetic waves are sustained due to the charges, but as soon as they enter the free space, they form closed loops and get radiated.

## B.3 Near and Far Field Regions

The field patterns, associated with an antenna, change with distance and are associated with two types of energy: - radiating energy and reactive energy. Hence, the space surrounding an antenna can be divided into three regions.

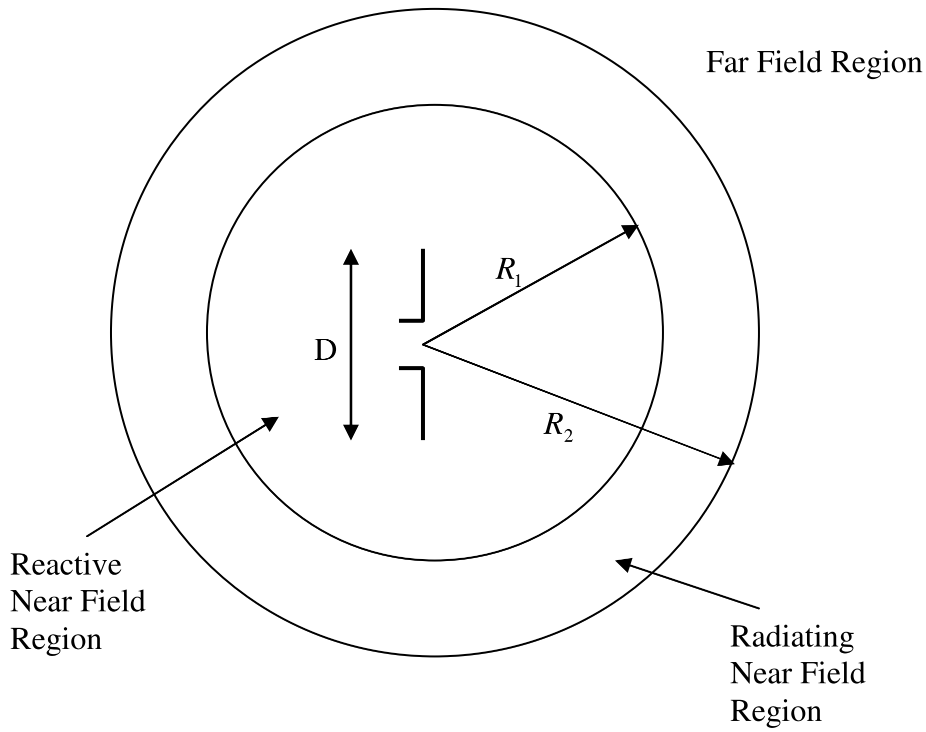


**Figure B. 2 Field regions around an antenna**

The three regions shown in Figure B.2 are [1] and [21]:

- Reactive near-field region: In this region, the reactive field dominates. The reactive energy oscillates towards and away from the antenna, thus appearing as reactance. In this region, energy is only stored and no energy is dissipated. The outermost boundary for this region is at a distance $R_1 = 0.62\sqrt{D^3/\lambda}$ where $R_1$ is the distance from the antenna surface, $D$ is the largest dimension of the antenna and $\lambda$ is the wavelength.
- Radiating near-field region (also called Fresnel region): This is the region which lies between the reactive near-field region and the far field region. Reactive fields are smaller in this field as compared to the reactive near-field region and the radiation fields dominate. In this region, the angular field distribution is a function of the distance from the antenna. The outermost boundary for this region is at a distance $R_2 = 2D^2/\lambda$ where $R_2$ is the distance from the antenna surface.

- Far-field region (also called Fraunhofer region): The region beyond the $R_2 = 2D^2 / \lambda$ is a far field region. In this region, the reactive fields are absent and only the radiation fields exist. The angular field distribution is not dependent on the distance from the antenna in this region and the power density varies as the inverse square of the radial distance in this region.

## B.4 Far field radiation from wires

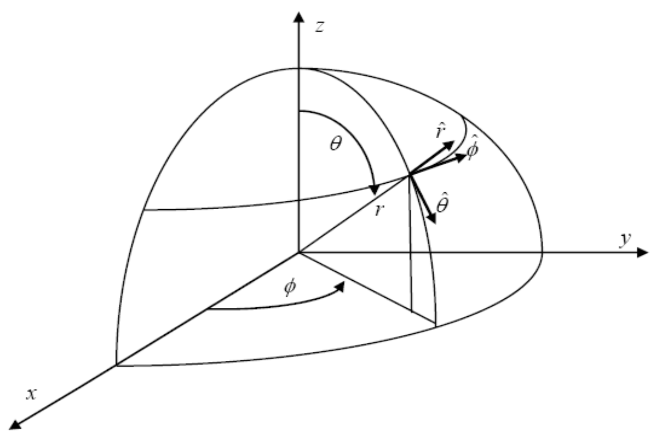


**Figure B. 3 Spherical co-ordinate systems for a Hertzian dipole**

The far field radiation from a Hertzian dipole can be conveniently explained with the help of the spherical co-ordinate system shown in Figure B.3. The z axis is taken to be the vertical direction and the xy plane is horizontal. θ denotes the elevation angle and φ denotes the azimuthal angle. The xz plane is the elevation plane (φ = 0) or the E-plane which is the plane containing the electric field vector and the direction of maximum radiation. The xy plane is the azimuthal plane (θ = π / 2) or the H-plane which is the plane containing the magnetic field vector and the direction of maximum radiation. The far field radiation can be explained with the help of the Hertzian dipole or infinitesimal dipole which is a piece of straight wire whose length L and diameter are both very small compared to one wavelength. A uniform current *I* (0) is assumed to flow along its length. If this dipole is placed at the origin along the z axis, then we can write [10]:

$$E_\theta = j\eta \frac{kI(0)Le^{-jkr}\sin\theta}{4\pi r}\left[1 + \frac{1}{jkr} - \frac{1}{(kr)^2}\right] \quad \text{(B.1)}$$

$$E_r = \eta \frac{I(0)Le^{-jkr}\cos\theta}{2\pi r^2}\left[1+\frac{1}{jkr}\right] \text{ ............................................ (B.2)}$$

$$H_\phi = j\frac{kI(0)Le^{-jkr}\sin\theta}{4\pi r}\left[1+\frac{1}{jkr}\right] \text{ ............................................ (B.3)}$$

$$H_r = 0 \text{ ............................................................. (B.4)}$$

$$H_\theta = 0 \text{ ............................................................. (B.5)}$$

$$E_\phi = 0 \text{ ............................................................. (B.6)}$$

For far field radiation, terms in $r^2$ and $r^3$ can be neglected; hence we can modify the above equations to write:

$$E_\theta = j\eta\frac{kI(0)Le^{-jkr}}{4\pi r}\sin\theta \text{ ................................................. (B.7)}$$

$$H_\phi = j\frac{kI(0)Le^{-jkr}}{4\pi r}\sin\theta \text{ ................................................. (B.8)}$$

$$E_r = 0 \text{ .................................................................. (B.9)}$$

where $\eta$ = intrinsic free space impedance

$k = 2\pi/\lambda$ $k$ = wave propagation constant

$r$ = radius for the spherical co-ordinate system.

In all the above equations, the phase term $e^{j\omega t}$ has been dropped and it is assumed that all the fields are sinusoidally varying with time. It is seen from the above equations that the only non-zero fields are $E_\theta$ and $H_\phi$, and that they are transverse to each other. The ratio $E_\theta / H_\phi = \eta$, such that the wave impedance is $120\pi$ and the fields are in phase and inversely proportional to *r*. The directions of *E, H* and *r* form a right handed set such that the Poynting vector is in the *r* direction and it indicates the direction of propagation of the electromagnetic wave. Hence the time average Poynting vector can be written as:

$$\mathbf{W}_{av} = \frac{1}{2}\mathrm{Re}\left[\mathbf{E}\times\mathbf{H}^*\right] \ (Watts/m^2) \text{ ............................................ (B.10)}$$

where *E* and *H* represent the peak values of the electric and magnetic fields respectively.
The average power radiated by an antenna can be written as:

$$P_{rad} = \oint\!\!\oint \mathbf{W}_{rad}\, d\mathbf{s} \quad (Watts) \text{ ............................................ (B.11)}$$

where $ds$ is the vector differential surface $= r^2 \sin\theta \, d\theta \, d\phi \, \hat{r}$

$W_{rad}$ is the magnitude of the time average Poynting vector ($Watts / m^2$)

The radiation intensity is defined as the power radiated from an antenna per unit solid angle and is given as:

$$U = r^2 \mathbf{W}_{rad} \quad \text{(B.12)}$$

where $U$ is the radiation intensity in Watts per unit solid angle.

### B.5 Antenna Performance Parameters

The performance of an antenna can be gauged from a number of parameters. Certain critical parameters are discussed below.

#### B.5.1 Radiation Pattern

The radiation pattern of an antenna is a plot of the far-field radiation properties of an antenna as a function of the spatial co-ordinates which are specified by the elevation angle $\theta$ and the azimuth angle $\phi$. More specifically it is a plot of the power radiated from an antenna per unit solid angle which is nothing but the radiation intensity. Let us consider the case of an isotropic antenna. An isotropic antenna is one which radiates equally in all directions. If the total power radiated by the isotropic antenna is $P$, then the power is spread over a sphere of radius $r$, so that the power density $S$ at this distance in any direction is given as:

$$S = \frac{P}{area} = \frac{P}{4\pi r^2} \quad \text{(B.13)}$$

Then the radiation intensity for this isotropic antenna $U_i$ can be written as:

$$U_i = r^2 S = \frac{P}{4\pi} \quad \text{(B.14)}$$

An isotropic antenna is not possible to realize in practice and is useful only for comparison purposes. A more practical type is the directional antenna which radiates more power in some directions and less power in other directions. A special case of the directional antenna is the omni-directional antenna whose radiation pattern may be constant in one plane (e.g. E-plane) and varies in an orthogonal plane (e.g. H-plane). The radiation pattern plot of a generic directional antenna is shown in Figure B.4.

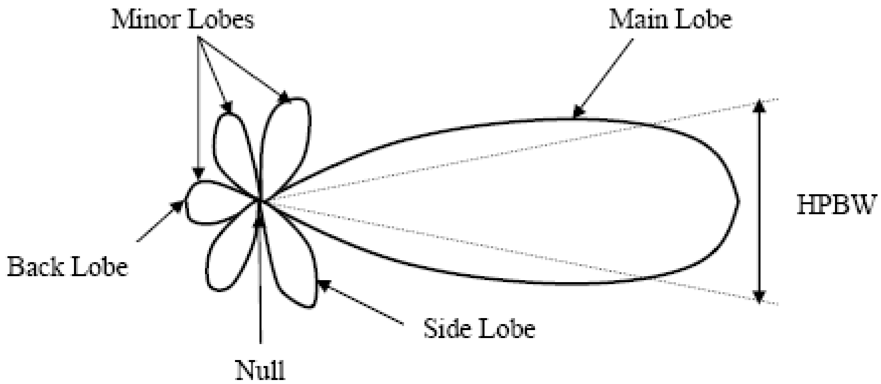


**Figure B. 4 Radiation pattern of a generic directional antenna**

Figure B.4 can be described as follows [21]:

- HPBW: The half power beam-width (HPBW) can be defined as the angle subtended by the half power points of the main lobe.
- Main Lobe: This is the radiation lobe containing the direction of maximum radiation.
- Minor Lobe: All the lobes other then the main lobe are called the minor lobes. These lobes represent the radiation in undesired directions. The level of minor lobes is usually expressed as a ratio of the power density in the lobe in question to that of the major lobe. This ratio is called as the side lobe level (expressed in decibels).
- Back Lobe: This is the minor lobe diametrically opposite to the main lobe.
- Side Lobes: These are the minor lobes adjacent to the main lobe and are separated by various nulls. Side lobes are generally the largest among the minor lobes.
- Front-to-Back ratio: It is the ratio of the maximum directivity in a forward direction to the directivity in a specified rearward direction. This ratio is expressed in dB.

In most wireless systems, minor lobes are undesired. Hence a good antenna design should minimize the minor lobes.

### B.5.2 Directivity

The directivity of an antenna has been defined as “the ratio of the radiation intensity in a given direction from the antenna to the radiation intensity averaged over all directions”

[10]. In other words, the directivity of a non isotropic source is equal to the ratio of its radiation intensity in a given direction, over that of an isotropic source.

$$D = \frac{U}{U_i} = \frac{4\pi U}{P} \quad \text{(B.15)}$$

where $D$ is the directivity of the antenna

$U$ is the radiation intensity of the antenna

$U_i$ is the radiation intensity of an isotropic source

$P$ is the total power radiated

Sometimes, the direction of the directivity is not specified. In this case, the direction of the maximum radiation intensity is implied and the maximum directivity is given by [8] as:

$$D_{\max} = \frac{U_{\max}}{U_i} = \frac{4\pi U_{\max}}{P} \quad \text{(B.16)}$$

where $D_{\max}$ is the maximum directivity

$U_{\max}$ is the maximum radiation intensity

Directivity is a dimensionless quantity, since it is the ratio of two radiation intensities. Hence, it is generally expressed in dBi. The directivity of an antenna can be easily estimated from the radiation pattern of the antenna. An antenna that has a narrow main lobe would have better directivity, than the one which has a broad main lobe, hence it is more directive.

### B.5.3 Input Impedance

The input impedance of an antenna is defined as "the impedance presented by an antenna at its terminals or the ratio of the voltage to the current at the pair of terminals or the ratio of the appropriate components of the electric to magnetic fields at a point". Hence the impedance of the antenna can be written as:

$$Z_{in} = R_{in} + jX_{in} \quad \text{(B.17)}$$

where $Z_{in}$ is the antenna impedance at the terminals

$R_{in}$ is the antenna resistance at the terminals

$X_{in}$ is the antenna reactance at the terminals

The imaginary part, $X_{in}$ of the input impedance represents the power stored in the near field of the antenna. The resistive part, $R_{in}$ of the input impedance consists of two components, the radiation resistance $R_r$ and the loss resistance $R_L$. The power associated with the radiation resistance is the power actually radiated by the antenna, while the power dissipated in the loss resistance is lost as heat in the antenna itself due to dielectric or conducting losses.

### B.5.4 Voltage Standing Wave Ratio (VSWR)

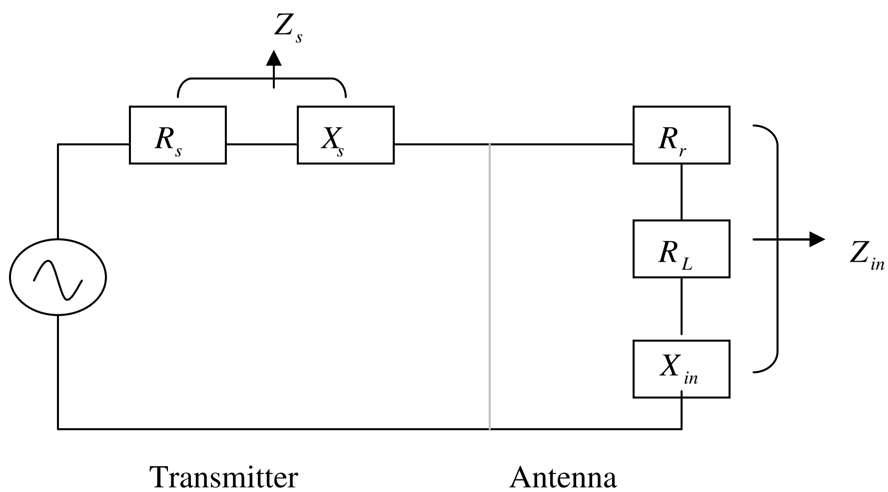


**Figure B. 5 Equivalent circuit of transmitting antenna**

In order for the antenna to operate efficiently, maximum transfer of power must take place between the transmitter and the antenna. Maximum power transfer can take place only when the impedance of the antenna ( $Z_{in}$ ) is matched to that of the transmitter ( $Z_s$ ). According to the maximum power transfer theorem, maximum power can be transferred only if the impedance of the transmitter is a complex conjugate of the impedance of the antenna under consideration and vice-versa. Thus, the condition for matching is:

$$Z_{in} = Z_s^* \qquad \text{(B.18)}$$

If the condition for matching is not satisfied, then some of the power maybe reflected back and this leads to the creation of standing waves, which can be characterized by a parameter called as the Voltage Standing Wave Ratio (VSWR).

The VSWR is given as:

$$VSWR = \frac{1+|\Gamma|}{1-|\Gamma|} \quad \text{(B.19)}$$

$$\Gamma = \frac{V_r}{V_i} = \frac{Z_{in} - Z_s}{Z_{in} + Z_s} \quad \text{(B.20)}$$

where $\Gamma$ is called the reflection coefficient

$V_r$ is the amplitude of the reflected voltage wave

$V_i$ is the amplitude of the incident voltage wave

The VSWR is basically a measure of the impedance mismatch between the transmitter and the antenna. The higher the VSWR, the greater is the mismatch. The minimum VSWR which corresponds to a perfect match is unity. A practical antenna design should have an input impedance of either $50\Omega$ or $75\Omega$ since most radio equipment is built for this impedance.

### B.5.6 Return Loss (RL)

Return loss is a measure of power reflected from imperfections in an electrical or optical communications link. It is the ratio of the power of the wave reflected from the imperfection to that of the incident wave. The return loss value describes the reduction in the amplitude of the reflected energy, as compared to the forward energy. As explained in the preceding section, reflection of waves leads to the formation of standing waves, when the transmitter and antenna impedance do not match. Hence the RL is a parameter similar to the VSWR to indicate how well the matching between the transmitter and antenna has taken place. The RL is given as [1]:

$$RL = 20\log_{10}|\Gamma| \qquad (dB) \quad \text{(B.21)}$$

For perfect matching between the transmitter and the antenna, $\Gamma = 0$ and $RL = \infty$ which means no power would be reflected back, whereas $\Gamma = 1$ has a $RL = 0\ dB$, which implies that all incident power is reflected. For practical applications, a VSWR of 2 is acceptable, since this corresponds to an $RL$ of -9.5 dB.

### B.5.7 Antenna Efficiency

The antenna efficiency is a parameter which takes into account the amount of losses at the terminals of the antenna and within the structure of the antenna. These losses are given as [1]:

- Reflections because of mismatch between the transmitter and the antenna
- $I^2R$ losses (conduction and dielectric)

Hence the total antenna efficiency can be written as:

$$e_t = e_r e_c e_d \quad \text{(B.22)}$$

where $e_t$ = total antenna efficiency

$e_r = (1 - |\Gamma^2|)$ = reflection (mismatch) efficiency

$e_c$ = conduction efficiency

$e_d$ = dielectric efficiency

Since $e_c$ and $e_d$ are difficult to separate, they are lumped together to form the $e_{cd}$ efficiency which is given as:

$$e_{cd} = e_c e_d = \frac{R_r}{R_r + R_L} \quad \text{(B.23)}$$

$e_{cd}$ is called as the antenna radiation efficiency and is defined as the ratio of the power delivered to the radiation resistance $R_r$, to the power delivered to $R_r$ and $R_L$.

### B.5.8 Antenna Gain

Antenna gain is a parameter which is closely related to the directivity of the antenna. We know that the directivity is how much an antenna concentrates energy in one direction in preference to radiation in other directions. Hence, if the antenna is 100% efficient, then the directivity would be equal to the antenna gain and the antenna would be an isotropic radiator. Since all antennas will radiate more in some direction than in others, therefore the gain is the amount of power that can be achieved in one direction at the expense of the power lost in the others. The gain is always related to the main lobe and is specified in the direction of maximum radiation unless indicated. It is given as [10]:

$$G(\theta,\phi) = e_{cd} D(\theta,\phi) \qquad (dB) \quad \text{(B.24)}$$

### B.5.9 Polarization

Polarization of a radiated wave is defined as "that property of an electromagnetic wave describing the time varying direction and relative magnitude of the electric field vector". The polarization of an antenna refers to the polarization of the electric field vector of the radiated wave. In other words, the position and direction of the electric field with reference to the earth's surface or ground determines the wave polarization. The most common types of polarization include the linear (horizontal or vertical) and circular (right hand polarization or the left hand polarization) [10].

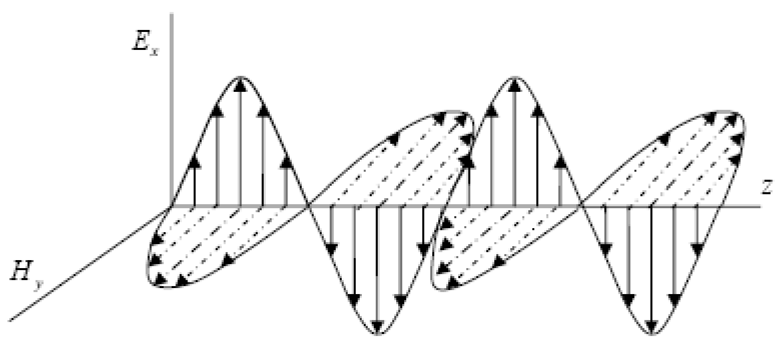


**Figure B. 6 A linearly (or vertically) polarized wave**

If the path of the electric field vector is back and forth along a line, it is said to be linearly polarized. Figure B.6 shows a linearly polarized wave. In a circularly polarized wave, the electric field vector remains constant in length but rotates around in a circular path. A left hand circular polarized wave is one in which the wave rotates counterclockwise whereas right hand circular polarized wave exhibits clockwise motion as shown in Figure B.7.

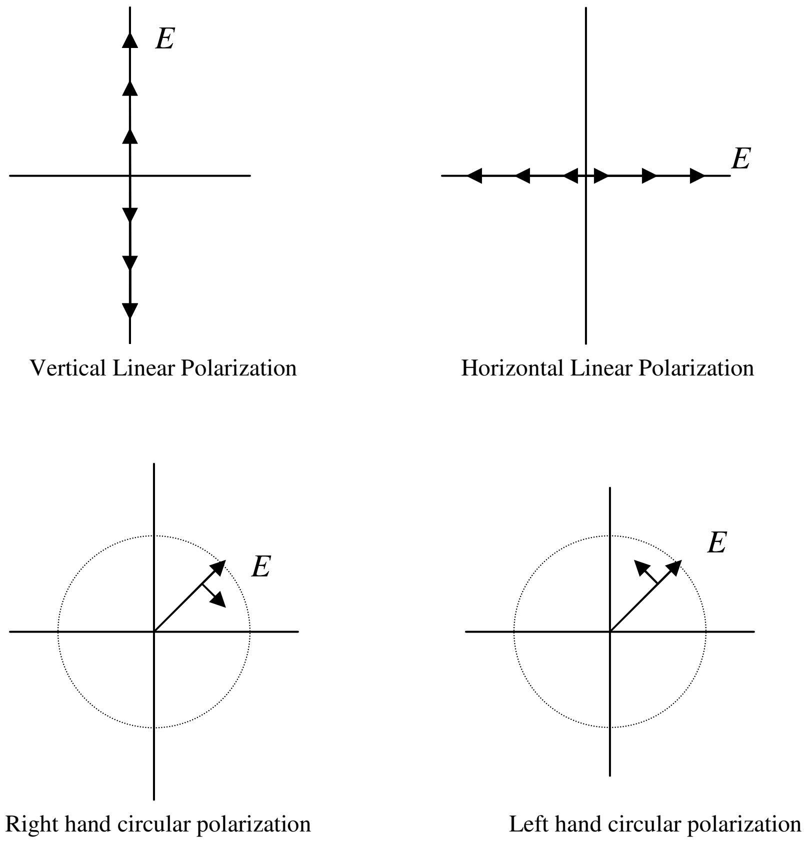


**Figure B. 7 Commonly used polarization schemes**

### Principal planes

For a linear polarized antenna, principal planes are E-plane and H-plane.

- **E-Plane**

For a linear polarized antenna, it is the plane containing the electric field vector and the direction of maximum radiation.

- **H-Plane**

For a linearly polarized antenna, it is the plane containing the magnetic field vector and the direction of maximum radiation.

## B.5.10 Bandwidth

The bandwidth of an antenna is defined as “the range of usable frequencies within which the performance of the antenna, with respect to some characteristic, conforms to a specified standard” [1]. The bandwidth can be the range of frequencies on either side of the center frequency where the antenna characteristics like input impedance, radiation pattern, beam-width, polarization, side lobe level or gain, are close to those values which have been obtained at the center frequency. The bandwidth of a broadband antenna can be defined as the ratio of the upper to lower frequencies of acceptable operation. The bandwidth of a narrowband antenna can be defined as the percentage of the frequency difference over the center frequency. These definitions can be written in terms of equations as follows:

$$BW_{broadband} = \frac{f_H}{f_L} \quad \text{(B.25)}$$

$$BW_{narrowband}(\%) = \left[\frac{f_H - f_L}{f_C}\right] * 100 \quad \text{(B.26)}$$

where $f_H =$ Upper frequency

$f_L =$ Lower frequency

$f_c =$ Center frequency

An antenna is said to be broadband if $\frac{f_H}{f_L} = 2$. One method of judging how efficiently an antenna is operating over the required range of frequencies is by measuring its VSWR or the return loss (RL). A $VSWR \leq 2 (RL \geq -9.5dB)$ [3] ensures good performance.

# References


1. C.A. Balanis, Antenna Theory: Analysis and Design, John Wiley & Sons, Inc, 1997
2. Kin-Lu Wong: Compact and Broad Band Microstrip Antennas, John Wiley & Sons, Inc, 2002
3. JR James & P S Hall, Handbook of Microstrip Antennas, Peter Peregrinus Ltd., 1989
4. Keith C. Huie, "Microstrip Antennas: Broadband Radiation Patterns Using Photonic Crystal Substrates", Thesis submitted to the Faculty of the Virginia Polytechnic Institute and State University in partial fulfillment of the requirements for the degree of MSc in Electrical Engineering Blacksburg, VA, 2002
5. Richard Q. Lee, Roberto Acosta, and J. S. Dahele, "Microstrip Antenna Array with Parasitic Elements", Prepared for the 1987 AP-S International Symposium sponsored by the IEEE Blacksburg, Virginia, June 15-17, pp. 1-6, 1987
6. Manish Kumar , Manish Kumar Sinha, L. K. Bandyopadhyay, Sudhir, Kumar. "Design of a Wideband Reduced Size Microstrip Antenna in VHF/Lower UHF Range", Central Mining Research Institute, Dhanbad; Instrumentation div., CMRI, Barwa Road, Dhanbad – 826 001, Jharkhand (India)
7. Richard Q. Lee and Roberto Acosta, J.S. Dahele and K.F. Lee, An Experimental Investigation of Parasitic Microstrip Antenna Arrays, Prepared for the 1987 symposium on Antenna Application cosponsored by the University of Illinois and the Rome Air Development Center, September 23-25, pp. 1-15, 1987
8. David M. Pozar: "Microwave Engineering", 3rd, John Wiley & Sons, Inc., 2005
9. Sean M. Duffy, Member, IEEE, "An Enhanced Bandwidth Design Technique for Electromagnetically Coupled Microstrip Antennas", pp. 161-164, IEEE Trans. on Antennas and Propagation, Vol. 48, No. 2, February 2000
10. Warren L. Stutzman, Gary A. Thiele, "Antenna theory and Design", New York John Wiley and Sons, Inc, 1989
11. D. M. Pozar, "A Microstrip Antenna Aperture Coupled to a Microstrip Line", Electronics Letters, Vol. 21, pp. 49-50, January 17, 1985.

12. D. M. Pozar, “A Review of Aperture Coupled Microstrip Antennas: History, Operation, Development, and Application”, Microwave Online System Company world wide web site, July 1996
13. David R. Jackson, Jeffery T. Williams and Donald R. Wilton, Chapter 9: Antennas II, Applied Electromagnetics Laboratory Department of Electrical and Computer Engineering, University of Houston, Houston, TX 77204-4005
14. Roger F. Harrington, “Time Harmonic Electromagnetic Fields” New-York, McGraw Hill, 1961
15. D. M. Pozar, “A Review of Bandwidth Enhancement Techniques for Microstrip Antennas”, pp. 157-166, in **Microstrip Antennas**, IEEE Press, 1995
16. T. Sudha , T. S. Vedavathy, “A Dual Band Circularly Polarized Microstrip Antenna with a Single Feed”, http://citeseer.ist.psu.edu/517634.html, cited June, 15, 2007
17. D.M. Pozar, B. Kaufman, “Increasing the Bandwidth of a Microstrip Antenna by Proximity Coupling”, Electron. Let, Vol. 23, No. 8, pp. 368-369, 1987
18. Sonnet User’s Manual, “Sonnet’s Users Guide” Release 11
19. V.B. Romodin, V.I. Oznobikhin, V.V. Kopylov, Scientific Research Institute om Electronic Devices, Novosibirsk, Russia, P.S. Hall //Microwave Journal. 1986. March, pp. 133-138
20. K. Solbach and O. Litschke, “Patch-Array-Antenna Feed Network Providing Bandwidth Improvement”, Gerhard-Mercator-Universität Duisburg, http://hft.uni-duisburg-essen.de/forschung/paper/MIOP-Antenne.pdf , cited July, 3,2007
21. Robert S. Elliot, Antenna Theory and Design, Prentice Hall, Englewood, 1981
22. S. Drabowitch, A. Paper, H. Griffiths, J. Encinas and Bradford L. Smith, Modern Antenna, University Press, Cambridge, 1998

## Declaration

I, the undersigned student, declare that this thesis work is my original work, has not been presented for a degree in this or any other universities, and all sources of materials used for the thesis work have been fully acknowledged.

Name: _Zewdu Hailu_ Signature: ____________

Place: Addis Ababa

Date of submission: January, 2008

This thesis has been submitted for examination with my approval as a university advisor.

Dr. Ing. Mohammed Abdo Signature: ____________

Advisor's Name